JOURNAL OF BACTERIOLOGY, Oct. 2006, p. 6899–6914 Vol. 188, No. 19
0021-9193/06/$08.00+0 doi:10.1128/JB.00690-06

The TadV Protein of *Actinobacillus actinomycetemcomitans* Is a Novel Aspartic Acid Prepilin Peptidase Required for Maturation of the Flp1 Pilin and TadE and TadF Pseudopilins†

Mladen Tomich,[1] Daniel H. Fine,[2] and David H. Figurski[1]*

Department of Microbiology, College of Physicians and Surgeons, Columbia University, New York, New York 10032,[1] *and Department of Oral Biology, University of Medicine and Dentistry of New Jersey, Newark, New Jersey 07103*[2]

Received 15 May 2006/Accepted 14 July 2006

The *tad* locus of *Actinobacillus actinomycetemcomitans* encodes genes for the biogenesis of Flp pili, which allow the bacterium to adhere tenaciously to surfaces and form strong biofilms. Although *tad* (*t*ight *ad*herence) loci are widespread among bacterial and archaeal species, very little is known about the functions of the individual components of the Tad secretion apparatus. Here we characterize the mechanism by which the pre-Flp1 prepilin is processed to the mature pilus subunit. We demonstrate that the *tadV* gene encodes a prepilin peptidase that is both necessary and sufficient for proteolytic maturation of Flp1. TadV was also found to be required for maturation of the TadE and TadF pilin-like proteins, which we term pseudopilins. Using site-directed mutagenesis, we show that processing of pre-Flp1, pre-TadE, and pre-TadF is required for biofilm formation. Mutation of a highly conserved glutamic acid residue at position +5 of Flp1, relative to the cleavage site, resulted in a processed pilin that was blocked in assembly. In contrast, identical mutations in TadE or TadF had no effect on biofilm formation, indicating that the mechanisms by which Flp1 pilin and the pseudopilins function are distinct. We also determined that two conserved aspartic acid residues in TadV are critical for function of the prepilin peptidase. Together, our results indicate that the *A. actinomycetemcomitans* TadV protein is a member of a novel subclass of nonmethylating aspartic acid prepilin peptidases.

Actinobacillus actinomycetemcomitans is a gram-negative, facultatively anaerobic coccobacillus that inhabits the oral cavities of humans and other mammals (4, 30, 52). *A. actinomycetemcomitans* is an opportunistic pathogen, primarily known as the etiologic agent of localized aggressive periodontitis, a particularly severe form of periodontal disease (3, 30). *A. actinomycetemcomitans* has also been associated with nonoral infections, including endocarditis, septicemia, and abscesses (77). We have identified a locus of 14 genes (*flp-1flp-2tadVrcp CABtadZABCDEFG*), designated the *tad* (*t*ight *ad*herence) locus, which is essential for the ability of the organism to adhere tenaciously to surfaces and form biofilms (40, 42, 59, 62). The *A. actinomycetemcomitans tad* locus is required for the biogenesis of long and bundled pili, termed Flp fibrils, which confer the tight adherence phenotype (35, 38, 40, 42). A functional *tad* locus is essential for colonization, persistence, and bone loss in a rat model of localized aggressive periodontitis (68), indicating that adherence is a critical component of the virulence repertoire of *A. actinomycetemcomitans*.

At least 12, and probably 13, of the genes in the *tad* locus are essential for Flp pilus biogenesis (40, 42, 59, 62). Certain components of the *A. actinomycetemcomitans* Flp pilus biogenesis system, including the RcpA predicted outer membrane secretin (29), the TadA ATPase (7), and the PilC-like TadB and TadC proteins (57), share similarity to those of bacterial type II secretion (T2S) and type IV pilus (T4P) systems, while TadA also has homology to the type IV secretion (T4S) system NTPases (39, 50, 61, 62). Other proteins comprising the Tad secretion apparatus, including RcpB, RcpC, TadD, and TadG, exhibit no significant amino acid sequence similarity to known components of bacterial secretion systems and cannot be assigned predicted functions.

A locus termed *cpa*, homologous to the *A. actinomycetemcomitans tad* genes, was identified in the nonpathogenic organism *Caulobacter crescentus* and is required for production of a polar pilus (70). We have identified highly conserved, homologous *tad* loci in a large number of diverse bacterial and archaeal species and have termed the locus the widespread colonization island (62). Recent studies have shown that there is a role for the *tad* locus in pathogenesis of a number of organisms, including *Haemophilus ducreyi* (6, 71), the etiologic agent of chancroid, and *Pasteurella multocida* (26), which causes fowl cholera. Furthermore, in vivo induction of *tadD* expression has been documented in the fish pathogen *Yersinia ruckeri* (23). A very recent report showed the involvement of *Pseudomonas aeruginosa* Flp pili in adherence to epithelial cells and biofilm formation (15). Despite growing evidence for the involvement of *tad* loci in the pathogenesis of a number of bacterial species, little is known about the molecular mechanisms by which the Tad protein secretion system functions.

We and others have previously shown that the Flp1 pilin functions as a major structural component of the *A. actinomycetemcomitans* Flp pili and that the mature pilin is a product of a proteolytically modified pre-Flp1 protein, encoded by *flp-1* (38, 42). Pilins and/or pilin-like proteins of other pilus biogenesis and protein secretion systems, such as the T4P and T2S systems, are cleaved (processed) by proteins termed prepilin

* Corresponding author. Mailing address: Department of Microbiology, College of Physicians and Surgeons, Columbia University, 1516 HHSC, 701 West 168th Street, New York, NY 10032. Phone: (212) 305-4579. Fax: (212) 305-1468. E-mail: dhf2@columbia.edu.

† Supplemental material for this article may be found at http://jb.asm.org/.

peptidases (20, 45, 64, 75). The predicted *tadV* gene product of *A. actinomycetemcomitans* has homology to T4P and T2S prepilin peptidases, and it represented a likely candidate to encode a Flp1 pilin-maturing enzyme. We have previously demonstrated that the *tadV* gene is essential for Flp pilus biogenesis (59). The *C. crescentus* CpaA protein, which is a homolog of *A. actinomycetemcomitans* TadV (62), has also been proposed to function as a prepilin peptidase (70). A very recent report has demonstrated the requirement of *P. aeruginosa* FppA protein, a TadV homolog, for Flp pilin maturation (15). However, this study did not directly analyze processing of the pilin by FppA.

The T4P and T2S prepilin peptidases also have homology to the proteases that process components of the DNA uptake apparatus in competence systems (12), as well as preflagellin peptidases in *Archaea* that are required for flagellar biogenesis (2, 6, 76). A study of the *Vibrio cholerae* TcpJ protein, which functions as a T4P prepilin peptidase, was the first to identify two conserved aspartic acid residues as the active sites for proteolysis (48). The corresponding aspartic acid residues have also been shown to be critical for function of other T4P prepilin peptidases (1, 48), preflagellin peptidases in *Archea* (5, 76), and the *P. aeruginosa* TadV homolog, FppA (15).

Pilin-like proteins, also known as "pseudopilins," are components of T4P and T2S systems in gram-negative bacteria, including those of *P. aeruginosa* and the T2S of *Klebsiella oxytoca* (8, 49, 64), as well as competence systems in gram-positive bacteria (19). The *K. oxytoca* Pul (63) and the *P. aeruginosa* Xcp (8) T2S systems require five distinct pseudopilins each. Although the precise roles of these proteins are unknown, it has been demonstrated that their processing by the cognate prepilin peptidases is critical for function (8, 11). Overexpression analysis of PulG, a *K. oxytoca* pseudopilin, has revealed that this protein can polymerize into an extracellular, pilus-like structure termed the pseudopilus (66). The same phenomenon occurs with the *Escherichia coli* homolog GspG (78). These observations support the hypothesis that pseudopilins form a periplasmic, piston-like structure that extrudes the substrate through intermittent rounds of polymerization and depolymerization (33). There is also evidence for a periplasmic pseudopilus in the *Xanthomonas campestris* Xps T2S system (36), as well as a DNA-importing pseudopilus on the membrane exterior in the competence system of *Bacillus subtilis* (10). It remains unclear what roles the pilin-like proteins play in bacterial pilus biogenesis, although it is likely that there is significant functional conservation between T4P and T2S pseudopilins.

Our laboratory is interested in elucidating the molecular pathway of Flp pilus biogenesis using *A. actinomycetemcomitans* as the model organism. As a key step in this process, we aimed to determine the molecular mechanism by which the Flp1 pilin is processed. Here we demonstrate that the TadV protein is the prepilin peptidase of the *A. actinomycetemcomitans* Tad system and that TadV is both necessary and sufficient for Flp1 pilin maturation. Moreover, we identify two additional substrates of the prepilin peptidase and show that the TadE and TadF pilin-like proteins are also processed by TadV. Given the architectural similarities of pre-TadE and pre-TadF to pre-Flp1 and that all three proteins require processing for function, TadE and TadF appear to be the first characterized members of a novel subclass of bacterial pseudopilins. We also show that two highly conserved aspartic acid residues in TadV are essential for function. Thus, the *A. actinomycetemcomitans* TadV protein is a member of a novel subclass of prepilin peptidases in bacteria.

MATERIALS AND METHODS

Bacterial strains, plasmids, and media. The bacterial strains and plasmids used in this study are listed in Table 1. *E. coli* strains were grown on Luria-Bertani (LB) agar plates or with aeration at 37°C in LB broth (65), supplemented with chloramphenicol (50 μg/ml) or kanamycin (50 μg/ml) as necessary. *A. actinomycetemcomitans* strains were grown as previously described (40). Briefly, cultures were grown on *A. actinomycetemcomitans* growth medium (AAGM) agar plates or in AAGM broth, each containing 0.75% glucose (wt/vol) and 0.4% sodium bicarbonate (wt/vol). Plates inoculated with *A. actinomycetemcomitans* were incubated for 48 to 72 h at 37°C in an atmosphere supplemented with 10% CO_2 (vol/vol), while broth cultures of *A. actinomycetemcomitans* were incubated at 37°C in tightly sealed culture tubes. AAGM agar plates or broth were supplemented with chloramphenicol (2 μg/ml), while nalidixic acid (20 μg/ml) was added to AAGM agar, as necessary.

Sequence analysis. The MacVector 7 software suite (Accelrys Inc.) was used to generate amino acid alignments using the ClustalW algorithm, as well as structural and antigenicity analyses. Homology searches were performed using the BLAST program available at http://www.ncbi.nlm.nih.gov. PSORTb 2.0 (http://www.psort.org) (27) and TMpred (34) algorithms were used to predict membrane localization, while TMpred alone was used to predict membrane topologies.

DNA manipulations. DNA-modifying enzymes, including restriction endonucleases and T4 DNA ligase, were obtained from New England Biolabs and used according to their instructions. Genomic DNA from *A. actinomycetemcomitans* was extracted using the DNeasy tissue kit (QIAGEN). DNA was amplified by PCR using Triple Master *Taq* (Eppendorf). Primer pairs used for PCR amplification of *A. actinomycetemcomitans flp-1*, *tadE*, *tadF*, and *tadV* genes, synthesized by Invitrogen, were as follows: *flp-1*-1BamHI (5′-GGATCCAACA ATAGGAGCATTAAGAC-3′) and *flp-1*-2 (5′-AGTTGTTATTTATTACTTAG TAAC-3′); *tadE*3-BamHI (5′-GGATCCAATAATATCGCCAGATAAAAAA AGG-3′) and *tadE*2 (5′-GCTTTAAATAATTGTAAATTGCC-3′); *tadF*3-BamHI (5′-GGATCCAGGCAATTTACAATTATTTAAAGC-3′) and *tadF*2 (5′-CTTAGATTATCGAGCAACTGCC-3′); *tadV*3-BamHI (5′-GGATCCTAG TTAGCAAAAGTAGCTAAA-AAATG-3′) and *tadV*2 (5′-CTGCTCATCAAG ACAATATTAG-3′). PCR products were ligated into the pCR2.1-TOPO or pCR4-TOPO TA cloning vectors (Invitrogen). Plasmid DNA was isolated using the QIAprep Spin miniprep kit (QIAGEN). Recombinant plasmids were introduced into *E. coli* by electroporation or $CaCl_2$ transformation (13). All constructs used in *A. actinomycetemcomitans* expression studies were generated in the pJAK17 broad-host-range IncQ vector (28; J. A. Kornacki, unpublished data). All genes were excised from the cloning vector as BamHI/EcoRI fragments, unless otherwise noted, and ligated into the corresponding sites in pJAK17. Plasmids were mobilized into *A. actinomycetemcomitans* strains using an *E. coli* donor strain, SK0140, which harbors an *oriT*-deficient derivative of plasmid RK2, which is not itself transferred efficiently (69).

For pre-Flp1 processing analysis in *E. coli*, the *tadV* gene was amplified using oligonucleotide primers AaUOBR1 (5′-CTATAGTTAGCAAAAGTAGCTAA AAAATG-3′) and AaUOCL1 (5′-CTGCTCATCAAGACAATATTAG-3′) and cloned into pCR2.1-TOPO. The *tadV* gene was then excised as a KpnI/XbaI fragment and cloned into the corresponding sites in plasmid pCF430, generating pSK305.

Site-directed mutagenesis. Specific amino acid substitutions in Flp1, TadE, TadF, and TadV proteins were generated by overlap extension PCR (32). In the first step, two fragments of the gene of interest, overlapping by approximately 20 nucleotides, were amplified separately using either a 5′-end or 3′-end primer (listed above) in combination with an internal primer. The overlapping regions of the two fragments contained the desired mutations, introduced through primer design. The two products were purified from agarose gels and were used as templates in a second PCR containing external primers. The overlapping regions of the two fragments from the initial amplification anneal and act both as a template and a primer for DNA synthesis, resulting in reconstitution of the full-length gene of interest containing the desired mutation. The mutant alleles were cloned into pJAK17, as described above.

Generation of chimeric proteins. The chimeric Flp1-TadE and Flp1-TadF expression constructs were made by fusing the sequence upstream of *flp-1* and its first 25 codons to the coding region of either mature *tadE* or *tadF*, starting with

TABLE 1. Bacterial strains and plasmids[a]

Strain or plasmid	Relevant characteristics	Reference or source
E. coli strains		
BL21	F^- *ompT hsdS*$_B$(r_B^- m_B^-) *gal dcm tonA*	Novagen
Top10	Cloning strain, F^- *mcrA* Δ(*mrr-hsdRMS-mcrBC*) ϕ80*lacZ*Δ*M15* Δ*lacX74 recA1 araD139* Δ(*ara-leu*)*7697 galU galK rpsL* (Str^r) *endA1 nupG*	Invitrogen
SK0140	Plasmid mobilization strain; Top10 with plasmid RK21761 (RK2*lac oriT*$^-$); Ap^r Km^r Tc^s Lac^+	69
MT1064	BL21 with pMT137 (*flp-1*); Cm^r	This work
MT1078	BL21 with pMT137 (*flp-1*) and pSK305 (*tadV*); Cm^r Tc^r	This work
A. actinomycetemcomitans strains		
CU1000N	Spontaneous nalidixic acid-resistant mutant of rough clinical isolate CU1000 (25), serotype f; Nal^r	40
DF2200N	Spontaneous nalidixic acid-resistant mutant of rough clinical isolate DF2200, serotype a; Nal^r	44
Aa0886	CU1000N *tadZ*Ω::IS*903*ϕ*kan*; Km^r Nal^r	62
Aa1332	CU1000N *tadB*Ω::IS*903*ϕ*kan*; Km^r Nal^r	40
Aa1347	CU1000N *tadE*Ω::IS*903*ϕ*kan*; Km^r Nal^r	40
Aa1354	CU1000N *rcpA*Ω::IS*903*ϕ*kan*; Km^r Nal^r	62
Aa1359	CU1000N *tadC*Ω::IS*903*ϕ*kan*; Km^r Nal^r	40
Aa1360	CU1000N *tadA*Ω::IS*903*ϕ*kan*; Km^r Nal^r	40
Aa1361	CU1000N *rcpC*Ω::IS*903*ϕ*kan*; Km^r Nal^r	62
Aa1512	CU1000N *tadF*Ω::IS*903*ϕ*kan*; Km^r Nal^r	40
Aa1561	CU1000N *tadG*Ω::IS*903*ϕ*kan*; Km^r Nal^r	40
Aa1577	CU1000N *tadD*Ω::IS*903*ϕ*kan*; Km^r Nal^r	40
Aa2508	Aa3074 with pGS-GFP-4; Cm^r Km^r Nal^r	This work
Aa2512	Aa1512 with pGS-GFP-4; Cm^r Km^r Nal^r	This work
Aa2513	Aa1512 with pMT115; Cm^r Km^r Nal^r	This work
Aa2515	Aa1512 with pMT127 (*tadF* E23A); Cm^r Km^r Nal^r	This work
Aa2519	CU1000N with pJAK17; Cm^r Km^r Nal^r	This work
Aa2530	JK1010 with pMT143 (*flp-1* E31A); Cm^r Km^r Nal^r	This work
Aa2531	Aa1512 with pJAK17; Cm^r Km^r Nal^r	This work
Aa2532	Aa1512 with pMT141 (wild-type *tadF*); Cm^r Km^r Nal^r	This work
Aa2534	Aa1347 with pJAK17; Cm^r Km^r Nal^r	This work
Aa2535	JK1010 with pMT137 (wild-type *flp-1*); Cm^r Km^r Nal^r	This work
Aa2536	JK1010 with pMT138 (*flp-1* G26A); Cm^r Km^r Nal^r	This work
Aa2540	Aa3074 with pJAK17; Cm^r Km^r Nal^r	This work
Aa2549	Aa1512 with pMT150 (*tadF* G18A); Cm^r Km^r Nal^r	This work
Aa2550	Aa1347 with pMT148 (*tadE* G10A); Cm^r Km^r Nal^r	This work
Aa2552	JK1010 with pMT156 (*flp-1* G26Y); Cm^r Km^r Nal^r	This work
Aa2553	Aa1347 with pMT157 (wild-type *tadE*); Cm^r Km^r Nal^r	This work
Aa2559	Aa2559 with pMT158 (*tadE* E15A); Cm^r Km^r Nal^r	This work
Aa2561	Aa3074 with pMT163 (*tadV* D77A); Cm^r Km^r Nal^r	This work
Aa2565	Aa3074 with pMT168 (*tadV* D23A); Cm^r Km^r Nal^r	This work
Aa2563	Aa1512 with pMT164 (*tadF* G18Y); Cm^r Km^r Nal^r	This work
Aa2567	Aa1347 with pMT169 (*tadE* G10Y); Cm^r Km^r Nal^r	This work
Aa2569	Aa3047 with pMT170 (wild-type *tadV*); Cm^r Km^r Nal^r	This work
Aa2575	Aa1347 with pMT176 (*flp-1-tadE* chimera); Cm^r Km^r Nal^r	This work
Aa2579	Aa1512 with pMT177 (*flp-1-tadF* chimera); Cm^r Km^r Nal^r	This work
Aa3074	DF2200N *tadV*::mini-Tn*5*Km; Km^r Nal^r	59
JK1010	CU1000N *flp-1*Ω::IS*903*ϕ*kan*; Km^r Nal^r	42
Plasmids		
pCF430	Broad-host-range IncP expression vector with arabinose-inducible promoter; *araC araBAD*p *lacI*^{q}; Tc^r	53
pCR2.1-TOPO	TA cloning vector; Ap^r Km^r	Invitrogen
pCR4-TOPO	TA cloning vector; Ap^r Km^r	Invitrogen
pGS-GFP-04	*gfp* cloned in pMMB207	31
pJAK17	Broad-host-range IncQ expression vector; derivative of pMMB67HE with Ω*cat* insertion in *bla*; *lacI*^{q} *tac*p mob^+; Cm^r	J. A. Kornacki, unpublished
pMT115	*tadF-egfp* fusion in pJAK17; Cm^r	This work
pMT127	*tadF* E23A in pJAK17; Cm^r	This work
pMT137	*flp-1* in pJAK17; Cm^r	This work
pMT138	*flp-1* G26A in pJAK17; Cm^r	This work
pMT141	*tadF* in pJAK17; Cm^r	This work
pMT143	*flp-1* E31A in pJAK17; Cm^r	This work
pMT148	*tadE* G10A in pJAK17; Cm^r	This work
pMT150	*tadF* G18A in pJAK17; Cm^r	This work
pMT156	*flp-1* G26Y in pJAK17; Cm^r	This work
pMT157	*tadE* in pJAK17; Cm^r	This work
pMT158	*tadE* E15A in pJAK17; Cm^r	This work
pMT163	*tadV* D77A in pJAK17; Cm^r	This work
pMT164	*tadF* G18Y in pJAK17; Cm^r	This work
pMT168	*tadV* D23A in pJAK17; Cm^r	This work
pMT169	*tadE* G10Y in pJAK17; Cm^r	This work
pMT170	*tadV* in pJAK17; Cm^r	This work
pMT176	*flp-1-tadE* chimera in pJAK17; Cm^r	This work
pMT177	*flp-1-tadF* chimera in pJAK17; Cm^r	This work
pSK305	*tadV* in pCF430; Tc^r	This work

[a]Abbreviations: Ap, ampicillin; Cm, chloramphenicol; Km, kanamycin; Nal, nalidixic acid; Tc, tetracycline.

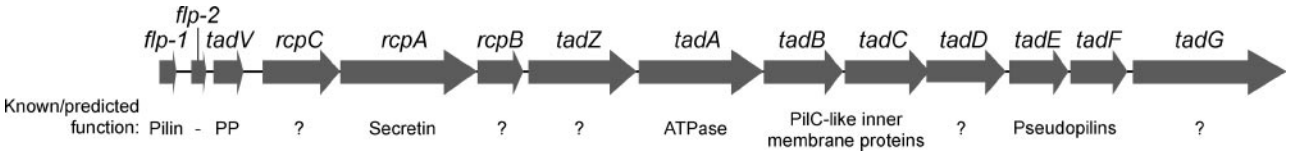

FIG. 1. The *tad* locus of *A. actinomycetemcomitans*. The position of each gene and the direction of transcription are indicated. The known or predicted functions of the *tad* locus gene products are indicated. The *flp-2* gene, predicted to encode a second pilin, is not expressed or required for pilus biogenesis in *A. actinomycetemcomitans*. Abbreviation: PP, prepilin peptidase.

the processing site at G(−1). The resulting chimeric proteins were $Flp1_{1-25}$-$TadE_{10-191}$ and $Flp1_{1-25}$-$TadF_{18-192}$, respectively. Both constructs have the *flp-1* Shine-Dalgarno site. The constructs were made using overlap extension PCR. In the first set of PCRs, we amplified using a downstream primer that was complementary to the sequence internal to *tadE* at its 5′ end (up to the glycine codon 10) or *tadF* (up to the glycine codon 18). We also amplified the *tadE* or *tadF* coding regions, starting with the glycine-encoding codons 10 and 18, respectively, using primers antiparallel to the downstream primers used to amplify the 5′ end of *flp-1*. Primers *tadE*2 and *tadF*2 (see above) were used for these reactions. The two products were then fused in a second round of PCR, using *flp-1*-1BamHI with either *tadE*2, to generate a *flp-1-tadE* fragment, or with *tadF*2, to generate a *flp-1-tadF* fragment. The chimeric genes were cloned into pCR2.1-TOPO and subsequently into pJAK17 as BamHI/EcoRI fragments to generate pMT176 and pMT177, respectively.

For the TadF-enhanced green fluorescent protein (eGFP) C-terminal fusion, the *tadF* gene was amplified with primers *tadF*3-BamHI (see above) and *tadF*4-NcoI (5′-CCATGGCTTTATTTGACCTGCCGGGATAT-3′) and cloned into pCR2.1-TOPO. The *tadE* gene was excised as a BamHI/NcoI fragment and cloned into the corresponding sites in the pEGFP vector (Clontech) to make the *tadF-egfp* in-frame fusion. The *tadF-egfp* fragment was excised with BamHI and EcoRI and cloned into the corresponding sites in pJAK17 to generate pMT115.

Preparation of semipure Flp1 pilin. To generate a Flp1-specific antiserum, the pilin protein was purified from Flp fibril preparations from *A. actinomycetemcomitans* strain CU1000N, as described by G. Schoolnik (67), with modifications by J. Kaplan and M. Tomich. Briefly, strain CU1000N was inoculated into five T-175 tissue culture flasks, containing 125 ml of AAGM broth. The flasks were incubated for 17 h with flask caps loosened. The biofilms were washed three times with phosphate-buffered saline, scraped, and resuspended in 150 mM ethanolamine, pH 10.5. Cells were then vortexed for 15 min to shear Flp pili and harvested by centrifugation at 20,000 × *g* for 35 min. The Flp1-enriched supernatant was collected and precipitated with 10% ammonium sulfate at 4°C for 17 h. Precipitated Flp fibrils were harvested by centrifugation at 10,000 × *g* and resuspended in 5 ml of ethanolamine. Ammonium sulfate precipitation was repeated two more times, and the final semipure Flp1 fraction was resuspended in 1 ml of ethanolamine.

Transmission electron microscopy of Flp pili. Flp pilus preparations were applied to Formvar-coated copper grids and briefly stained with 1% uranyl acetate. Samples were analyzed at the New York Structural Biology Center in an FEI Tecnai TF20 microscope at 80 kV.

Generation of Flp1 and TadE antisera. To increase purity of the pilin, the semipure Flp1 fraction was boiled for 30 min in Laemmli buffer (47) to dissociate fibrils into monomeric Flp1. The Flp1 fraction was separated by 18% sodium dodecyl sulfate-polyacrylamide gel electrophoresis (SDS-PAGE) and briefly stained with Coomassie blue, and the pilin monomers were excised and used to generate rabbit polyclonal antisera at Invitrogen. The TadE antiserum was generated using the $TadE_{177-191}$ peptide (EFNRSKFQYPGRSNK) conjugated to the keyhole limpet hemocyanin carrier protein. The resulting protein was used to generate a specific antiserum in rabbits at Sigma-Genosys. The antiserum was enriched for TadE peptide-specific antibodies by affinity purification, using a HiTrap NHS column (Amersham Biosciences) following the manufacturer's protocol.

Immunoblot analysis. *A. actinomycetemcomitans* strains were grown in 10 ml of AAGM broth for 17 h. Cultures were centrifuged to harvest bacterial cells, and the pellets were resuspended and boiled in Laemmli buffer (47). Equal amounts of protein from each strain were resolved by SDS-PAGE and analyzed by blotting with anti-Flp1 (1:20,000), anti-TadE (1:5,000), anti-GFP (1:10,000; Rockland Immunochemicals), or anti-T7 epitope tag antibody (1:5,000; Novagen). An anti-rabbit immunoglobulin G antibody (Sigma), conjugated to horseradish peroxidase (HRP), was used as a secondary antibody at a dilution of 1:50,000. For anti-GFP blots, an anti-goat immunoglobulin G secondary antibody, conjugated to HRP, was used at a dilution of 1:10,000 (Roche). Femto Western chemiluminescence reagent (Pierce) was used as substrate for HRP.

Processing of pre-Flp1 by TadV in *E. coli*. A culture of the *E. coli* BL21-derived strain MT1078, harboring pMT137 (*tac*p-*flp-1*) and pSK305 (*araBAD*p-*tadV*), grown in 5 ml of LB broth, supplemented with chloramphenicol and tetracycline, was used to inoculate three identical cultures in 5 ml each of fresh medium by 100-fold dilution. The cultures were grown to an optical density at 600 nm of approximately 0.8, which was designated the "0′" time point. At this point, a sample was collected from one of the cultures for immunoblot analysis. Cultures were supplemented with either isopropyl-β-D-thiogalactopyranoside (IPTG) or L-arabinose, or both, to induce *flp-1* and *tadV* expression, respectively. Cultures receiving IPTG were induced at the "0′" time point, while arabinose was added at 30 min post-IPTG induction, to allow accumulation of pre-Flp1. After sampling, bacterial cells were harvested, and the cell pellet was resuspended and boiled for 5 min in Laemmli buffer. Samples were normalized by taking absorbance readings at 280 nm and loading equivalent total protein amounts on gels for immunoblot analysis.

Adherence assays. Adherence of *A. actinomycetemcomitans* was examined both qualitatively and quantitatively. For the qualitative assay, stationary-phase cultures were subcultured into a 24-well microtiter dish containing 1 ml of AAGM per well supplemented with chloramphenicol and 1 mM IPTG. The strains were grown for 20 h, after which the medium was removed, and wells were washed five times with water. To visualize bacterial biofilms, 200 μl of a 0.5-mg/ml solution of ethidium bromide in water was added to each well and washed five times with water to remove unbound ethidium bromide. Biofilms were visualized under UV illumination.

The quantitative method is a modified protocol of the assay described by O'Toole and Kolter (43, 54). Briefly, 25 μl each of stationary-phase cultures of *A. actinomycetemcomitans* was used to inoculate wells of a 96-well microtiter dish, each containing 100 μl of AAGM. IPTG was either omitted or added to a final concentration of 0.1 mM or 1 mM. Strains were grown for 20 h to allow biofilm formation. Microtiter dishes were then washed vigorously 15 times with water to remove nonadherent bacteria. Biofilms were stained with 25 μl of 1% crystal violet per well. After 15 min, biofilms were washed 15 times with water and 200 μl of dimethyl sulfoxide was added to each well. Following a 90-minute incubation, 100 μl was transferred to a new 96-well microtiter dish, and the absorbance at 590 nm was determined in a Molecular Devices SpectraMax 340PC plate reader.

RESULTS

TadV is required for Flp1 processing in *A. actinomycetemcomitans*. The *A. actinomycetemcomitans tad* locus comprises 14 genes (Fig. 1), at least 12 of which are essential for Flp pilus biogenesis (40–42, 59, 62). The *A. actinomycetemcomitans* Flp1 pilin is the major structural component of Flp pili and is generated by processing of the prepilin encoded by the *flp-1* gene (38, 42). It has been shown that the pre-Flp1 protein is cleaved at a site following a glycine residue, which is part of a highly conserved processing site found in Flp1 pilin homologs, the consensus of which is G/XXXXEY (38, 42), where the forward slash indicates the processing site. The site also closely resembles the G/XXXXE processing site found in T2S, T4P and natural competence system pseudopilins (18, 24, 75), and T4P pilins (73). To further characterize the maturation and function of Flp1, we generated antiserum to the Flp1 monomer,

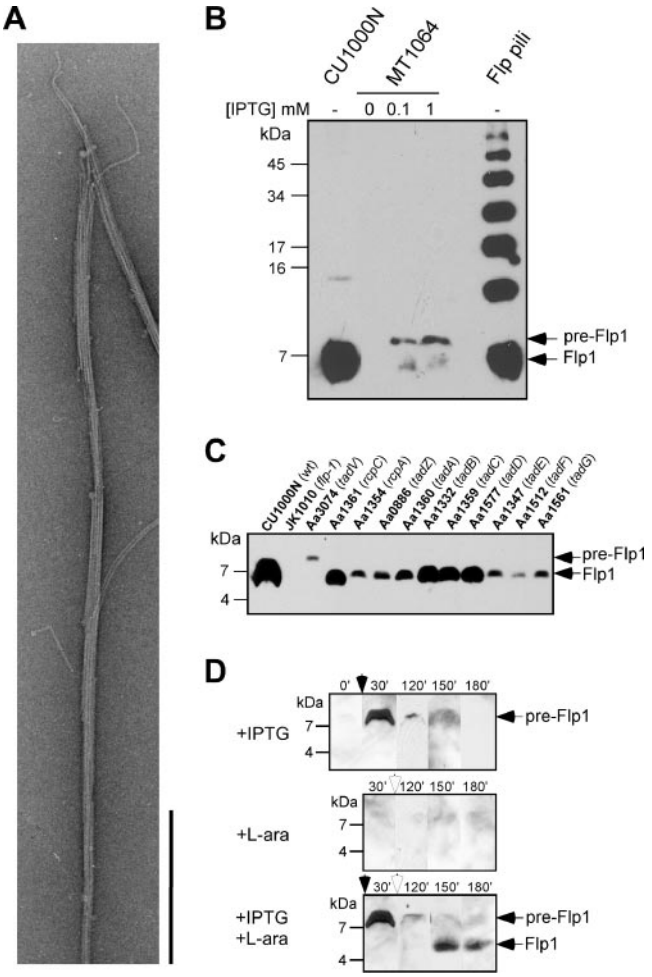

FIG. 2. Analysis of Flp1 expression and processing. (A) Transmission electron micrograph of the semipure Flp pilus preparation from *A. actinomycetemcomitans* CU1000N, stained with uranyl acetate. Bar, 300 nm. (B) Immunoblot analysis of Flp1 pilin expression in *A. actinomycetemcomitans* wild-type strain CU1000N and *E. coli* strain BL21 harboring the *tac*p–*flp-1* expression construct (strain MT1064) and pilin oligomerization in the semipure Flp pilus preparation. Strain MT1064 was grown in the absence or presence of either 0.1 mM or 1 mM IPTG, as indicated. (C) Flp1 expression and processing in *A. actinomycetemcomitans* nonpolar *tad* mutant strains. (D) Processing of pre-Flp1 by TadV in *E. coli* strain BL21. IPTG and/or L-arabinose (L-ara) was added as indicated left of the panel to induce expression of pre-Flp1 or TadV, respectively. Cultures were continuously sampled over a 3-h time course, and the levels and processing state of Flp1 were analyzed by anti-Flp1 immunoblotting. The numbers at the top of the panels indicate time (in minutes) post-IPTG induction. The black arrows at the top of the panels indicate the time of IPTG addition, whereas white arrows indicate the addition of L-arabinose. The positions of the pre-Flp1 prepilin and the mature Flp1 pilin are indicated with arrows on the right.

obtained from semipure pilus preparations of *A. actinomycetemcomitans* strain CU1000N. Purification of the pili was confirmed by transmission electron microscopy. Bundles of long Flp pili, strongly resembling those previously observed in association with wild-type *A. actinomycetemcomitans* strains (40), were abundant in the semipure pilus fraction (Fig. 2A).

To examine Flp1 expression in *A. actinomycetemcomitans*, whole-cell extracts of wild-type strain CU1000N were analyzed by immunoblotting with the anti-Flp1 antiserum. An abundant band of approximately 7 kDa was detected in strain CU1000N, corresponding in size to the processed pilin (Fig. 2B). Although the predicted molecular mass of mature Flp1 is 5.1 kDa, we have determined that Flp1 in strain CU1000N is glycosylated (data not shown), as has been previously documented for at least one other isolate of *A. actinomycetemcomitans* (37). Carbohydrate moieties on Flp1 likely contribute to the slightly reduced gel mobility of Flp1. The level of Flp1 glycosylation may be heterogeneous, which would also contribute to the width of the Flp1 band.

To further examine Flp1 processing, the full-length pilin was expressed in *E. coli* strain BL21 from plasmid pMT137 harboring the *flp-1* gene under the control of the *tac*p promoter (strain MT1064). A band of approximately 8 kDa, exactly matching the predicted molecular mass of the Flp1 prepilin, was identified in whole-cell extracts of strain MT1064 induced with either 0.1 mM or 1 mM IPTG, but not in its absence. The pre-Flp1 protein expressed in *E. coli* appeared to be unstable, as apparent degradation products were observed below the pre-Flp1 band (Fig. 2B). The detection of pre-Flp1 in *E. coli* strain MT1064, but not in strain CU1000N, confirmed that the prepilin is posttranslationally cleaved in *A. actinomycetemcomitans*.

We also analyzed semipure preparations of Flp pili by immunoblotting with anti-Flp1. Under standardized sample preparation conditions that include resuspension in Laemmli buffer containing 0.1% SDS and boiling for 5 min, the interactions between Flp-1 pilin monomers were not fully disrupted (Fig. 2B). Although the 7-kDa band corresponding to the monomeric Flp1 was the most abundant, bands corresponding to pilin oligomers were readily detectable (Fig. 2B). The disruption of Flp1 oligomers was not significantly more efficient when the Flp pilus preparations were boiled for up to 30 min (data not shown), indicating that the interactions between Flp1 monomers are extremely strong.

To examine Flp1 expression in *A. actinomycetemcomitans*, whole-cell extracts of strain CU1000N and nonpolar *tad* locus mutants (40, 42, 59, 62) were analyzed by immunoblotting with the anti-Flp1 antiserum. The *tad* mutant panel does not include a *flp-2* mutant, since this gene is not required for Flp pilus expression, or a mutant in the *rcpB* gene, which is essential for viability in the context of a functional *tad* locus (59). All of the mutants tested have been shown to be defective in Flp pilus biogenesis and biofilm formation and are complementable (40, 42, 59, 62). An abundant band of approximately 7 kDa, corresponding in size to mature Flp1, was detected in wild-type strain CU1000N and was absent in the *flp-1* mutant strain JK1010 (Fig. 2C). Flp1 was detectable in all other *tad* mutant backgrounds, although the levels of the pilin were variable. An approximately 8-kDa band, corresponding to unprocessed Flp1, was detected in the *tadV* strain Aa3074. Complementation of the *tadV* mutant strain with a wild-type copy of the *tadV* gene in *trans* restored pilus production and adherence (59), as well as Flp1 processing (see Fig. 7C, below), demonstrating that the TadV protein is required for processing of the Flp1 pilin.

Gel mobility of Flp1 was also altered in the *A. actinomycetemcomitans rcpC* mutant strain, with the pilin migrating at a slightly lower molecular weight relative to that in other *tad*

mutant backgrounds (Fig. 2C). The observed subtle difference in mobility of Flp1 in the *rcpC* mutant was reproducible and may indicate that the RcpC protein plays a role in posttranslational modification of the pilin. Levels of Flp1 in the whole-cell extracts of all of the *tad* mutants were reduced, albeit to various degrees, relative to pilin levels in the wild-type strain CU1000N preparation (Fig. 2C). The lowest levels of Flp1 were detected in the *tadV* and *tadF* mutant strains, in which the amounts of the prepilin or pilin, respectively, were reduced approximately 100-fold or more. A drastic reduction in Flp1 levels was also observed in extracts from *rcpA*, *tadZ*, *tadA*, *tadE*, and *tadG* mutant strains. The mutants that were affected the least were *rcpC*, *tadB*, *tadC*, and *tadD*, which exhibited an approximately twofold reduction in pilin abundance.

TadV is sufficient for pre-Flp1 processing. The requirement of the *tadV* gene for Flp1 processing in *A. actinomycetemcomitans* strongly indicates that the TadV protein is a prepilin peptidase. To examine if TadV can function as a Flp1-maturing protease and to determine if it is sufficient for processing of pre-Flp1, the two proteins were expressed in *E. coli* strain BL21 from compatible plasmids. The pre-Flp1 protein was expressed from the pJAK17-derived plasmid pMT137, which harbors the *flp-1* gene under the control of the *tac*p promoter. TadV was expressed from pCF430-derived plasmid pSK305, which harbors the *tadV* gene under the control of the arabinose-inducible *araBAD*p promoter. Three identical exponential-phase cultures of the *E. coli* strain MT1078 carrying both compatible plasmids were induced with either IPTG or arabinose, or both. To allow pre-Flp1 expression and accumulation, IPTG was added at the initial time point (0′) and arabinose was added 30 min later (Fig. 2D). Cultures were sampled over a 3-h time course, and the whole-cell extracts were analyzed by immunoblot analysis for expression and processing of Flp1.

An 8-kDa band, corresponding to pre-Flp1, was observed 30 min postinduction (Fig. 2D) in both cultures induced with IPTG. However, the pre-pilin appeared to be unstable in *E. coli* and was barely detectable at 120 min postinduction. This result was also observed in the *E. coli* strain BL21 harboring both pMT137 and the pCF430 vector (data not shown), indicating that degradation of pre-Flp1 is independent of *tadV* expression. Flp-1 was not detectable in strain MT1078 induced with arabinose alone (Fig. 2D). When IPTG and subsequently arabinose were added to the culture to induce expression of both pre-Flp1 and TadV, respectively, a band of approximately 5 kDa was detected at 150 and 180 min postinduction with IPTG (Fig. 2D). The lower-molecular-mass band matches exactly the predicted molecular mass of mature Flp1 pilin. The detection of mature Flp1 was absolutely dependent on *tadV* expression, demonstrating that the TadV protein is a prepilin peptidase sufficient for processing of the pre-Flp1 prepilin.

Architectural similarities between the TadE and TadF proteins and the Flp1 pilin. Initial analyses of the *A. actinomycetemcomitans tadE* and *tadF* gene products revealed that the two proteins exhibit 22% identity and 38% similarity at the amino acid sequence level (60). Amino acid alignment of *A. actinomycetemcomitans* TadE and TadF proteins, as well as their homologs encoded by *tad* loci of *H. ducreyi* (GenBank accession no. NC_002940), *P. multocida* (51), and *Y. pestis* (17), revealed a significant level of primary sequence similarity (Fig. 3A). The similarities between *A. actinomycetemcomitans* TadE and the homologous proteins from the listed organisms range between 45% and 70%, while similarities between TadF homologs range from 42% to 71%. Despite a relatively broad range of similarity levels within the TadE or TadF protein subclasses, certain amino acid residues are highly conserved in both groups. Of particular interest are those predicted to contain N-terminal signal sequences, flanked by a highly conserved sequence, GXXXXEF (Fig. 3A) (60), which strongly resembles the consensus processing site in the pre-Flp1 subfamily of prepilins (G/XXXXEY) (42), including the *A. actinomycetemcomitans* pre-Flp1 prepilin (Fig. 3A). However, neither TadE nor TadF exhibits significant primary sequence similarities to Flp1 outside of the putative N-terminal processing sites.

The domain architectures of *A. actinomycetemcomitans* TadE and TadF proteins exhibit striking similarity not only to that of each other, but also to that of the *A. actinomycetemcomitans* Flp1 pilin. In all three proteins the signal sequences, ranging in length from 10 (TadE) to 26 (Flp1) amino acids, are followed by a 20- to 25-amino-acid hydrophobic domain (Fig. 3B). In type IV pilins, such a domain is known to function as a transmembrane (TM) domain, transiently localizing the type IV pilins to the inner membrane and mediating interactions between pilin monomers as they are incorporated into the helical pilus structure (14, 55). TadE, TadF, and Flp1 all have a C-terminal β-sheet-rich domain, as predicted by multiple algorithms in the MacVector sequence analysis software. TadE and TadF both possess an additional α-helix-rich domain, absent in Flp1, that separates the hydrophobic region from the β-sheet-rich domain (Fig. 3B).

TadV is required for processing of the *A. actinomycetemcomitans* TadE and TadF pseudopilins. Given the presence of highly conserved processing sites in the N termini of the *tadE* and *tadF* gene products, we were interested in determining if TadE and/or TadF was posttranslationally processed like pre-Flp1. A peptide antibody was generated to a unique C-terminal portion of TadE and was used to probe whole-cell extracts of the *A. actinomycetemcomitans* wild-type strain CU1000N and the *tad* gene mutants. A band of approximately 20 kDa was identified in preparations from the wild-type strain CU1000N, which matches the predicted molecular mass of 20.5 kDa for the mature TadE protein processed at residue G10 (Fig. 3A and 4A). The TadE band was absent in the *tadE* mutant strain (Aa1347) (Fig. 4A). A band of approximately 22 kDa was detected in the *tadV* mutant strain Aa3074, matching the predicted molecular mass of the full-length *tadE* gene product of 21.6 kDa. Complementation of the *tadV* mutant strain with a wild-type *tadV* gene in *trans* restored pre-TadE processing (data not shown). These results indicate that the pre-TadE protein, encoded by *tadE*, is proteolytically modified and that the TadV prepilin peptidase is required for this process.

The *tadV* mutant strain was the only *tad* mutant blocked in processing of pre-TadE (Fig. 4A). The level of unprocessed TadE in the *tadV* mutant strain was consistently reduced, suggesting that proteolytic modification increases its stability in *A. actinomycetemcomitans*. The TadE protein was not detectable in the *tadF* mutant strain Aa1512 (Fig. 4A), even when immunoblots were overexposed (data not shown). Mature TadE was detected in preparations from all remaining *tad* mutant strains, albeit at varied levels. Of the strains expressing mature TadE, its levels were most drastically reduced in *rcpC* and *rcpA* mu-

FIG. 3. (A) Amino acid sequence alignment of *A. actinomycetemcomitans* TadE and TadF proteins and representative homologs encoded by *tad* loci in other bacterial species. The processing site of the Flp1 protein of *A. actinomycetemcomitans* is also aligned. Identical and similar residues are shown in darkly and lightly shaded boxes, respectively. Highly conserved G(−1) and E(+5) residues in the processing sites of the proteins are shown in black boxes. The arrow indicates the processing site. Abbreviations: Aact, *A. actinomycetemcomitans*; Hduc, *H. ducreyi*; Pmul, *P. multocida*; Ypes, *Y. pestis*. (B) Schematic diagrams of domain organization of the pre-TadF, pre-TadE, and pre-Flp1 proteins of *A. actinomycetemcomitans*. The signal peptide and hydrophobic domains, as well as portions of the proteins predicted to predominantly have either an α-helical or β-sheet structure, are indicated. The processing sites are indicated with black arrows. (C) Alignment of predicted Shine-Dalgarno sequences upstream of *A. actinomycetemcomitans* CU1000N *flp-1*, *tadE*, and *tadF* genes. Residues shown in bold are identical to the predicted *A. actinomycetemcomitans* Shine-Dalgarno sequence. The start codons are shown in bold on a shaded background.

tants (Fig. 4A), which exhibited an approximately 10-fold decrease in TadE abundance relative to the wild-type strain CU1000N. The *tadZ*, *tadA*, *tadC*, *tadD*, and *tadG* mutants exhibited a moderate decrease in TadE abundance. Only the *flp-1* and *tadB* mutants exhibited wild-type levels of TadE. Conversely, the observed decreases in TadE abundance in other *tad* mutant strains indicate that the proteins encoded by these genes directly or indirectly impact the stability of the TadE protein.

To examine the expression and processing of TadF, multiple attempts were undertaken to generate a TadF-specific antiserum. A recombinant His_6-TadF fusion protein was purified from *E. coli* and used as an antigen in hyperimmunizations (data not shown). However, the resulting antisera were unable to detect the TadF protein. It is possible that the low immunogenicity of TadF, predicted by multiple algorithms in the MacVector 7 sequence analysis software, resulted in an antiserum with low specificity for the TadF protein. In the absence of a functional anti-TadF antiserum, we fused the phage T7 epitope tag (MASMTGGQQMG) to the C terminus of TadF to analyze its expression and processing in *A. actinomycetemcomitans*. The resulting protein, designated TadF-T7, was functional and able to partially complement adherence of the *A. actinomycetemcomitans tadF* mutant strain Aa1512 (data not

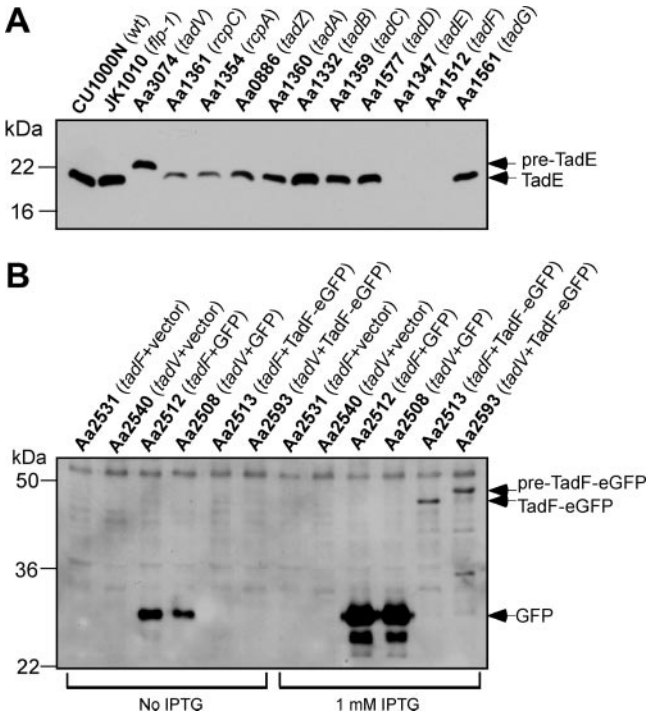

FIG. 4. Analysis of expression and processing of the TadE (A) and TadF (B) pseudopilins. (A) Whole-cell extracts of nonpolar *tad* mutants of *A. actinomycetemcomitans* were prepared and analyzed by anti-TadE immunoblotting. The positions of pre-TadE and mature TadE protein bands are indicated by black arrows. (B) Analysis of TadF-eGFP expression and processing. The *tadF* and *tadV* mutants of *A. actinomycetemcomitans* harboring either the vector control, a GFP-encoding plasmid, or the TadF-eGFP expression construct were grown in the absence or presence of IPTG, as indicated below the panel. Whole-cell extracts were immunoblotted using the anti-GFP antibody. The black arrows indicate the positions of pre-TadF-eGFP, TadF-eGFP, and GFP.

shown). Despite clear evidence for expression of TadF-T7 provided by phenotypic complementation, we were unable to detect the fusion protein by immunoblotting using an anti-T7 epitope tag monoclonal antibody (data not shown), indicating that a low level of TadF is sufficient for function in *A. actinomycetemcomitans*.

Fusing a protein with a high turnover rate to a stable polypeptide can lead to increased stability of the chimera, relative to the native protein (16). One such potential fusion partner is GFP, which is highly stable under a variety of conditions (9). To examine TadF expression and processing, eGFP was fused to the C terminus of TadF. The *tadF* mutant harboring the TadF-eGFP expression construct (Aa2513) formed a biofilm in the qualitative assay and exhibited a similar level of adherence to the wild-type strain in the quantitative assay, both in the absence and presence of IPTG (see Fig. S1 in the supplemental material). These results indicate that the TadF-eGFP fusion protein is functional. In contrast, the *tadF* mutant strain with either the pJAK17 vector or the pGS-GFP-4 plasmid did not exhibit adherence in the quantitative assay (data not shown). Despite complementation of adherence, the TadF-eGFP fusion strain did not exhibit fluorescence, while cells of the *tadF* mutant strain with the control plasmid pGS-GFP-4 (Aa2512) were fluorescent (data not shown). The absence of fluorescence of the TadF-eGFP protein suggests that the C terminus of TadF localizes to the periplasmic space (22), which is consistent with its predicted membrane topology.

To examine if the TadF protein is processed, expression of the TadF-eGFP fusion construct in the *tadV* mutant strain (Aa2593) was examined by immunoblotting with an anti-GFP monoclonal antibody. The GFP protein was detectable in both the *tadF* and *tadV* mutant strains carrying pGS-GFP-4, but it was not detectable in the mutants with the pJAK17 vector alone (Fig. 4B). In the presence of 1 mM IPTG, but not in its absence, a band of approximately 46 kDa was identified in preparations of the *tadF* mutant strain complemented with the TadF-eGFP (Aa2513). The TadF-eGFP band matches the predicted molecular mass of 46.5 kDa, which corresponds to the fusion protein processed after residue G18 (Fig. 3A and 4B). A higher-molecular-mass band of approximately 49 kDa was identified in the preparation from the *tadV* mutant strain expressing TadF-eGFP, which closely matches the predicted molecular mass of 48.7 kDa of the uncleaved fusion protein. These results demonstrate that the TadF-eGFP fusion protein is processed by a TadV-dependent mechanism. Given the similar architectures of the pre-Flp1, pre-TadE, and pre-TadF proteins and that all three proteins are processed by the TadV prepilin peptidase, we designate the *A. actinomycetemcomitans* TadE and TadF proteins as "pseudopilins" and their immature forms as "prepseudopilins." The *A. actinomycetemcomitans* TadE and TadF pseudopilins do not exhibit significant homology to any of the known pseudopilins from T4P, T2S, or natural competence systems, while they are highly conserved within the *tad* loci (62). Therefore, TadE and TadF appear to be members of a novel subclass of pseudopilins required for bacterial pilus assembly.

Expression analyses of the TadE and TadF pseudopilins. To further examine the functional similarities between the Flp1 pilin and the TadE and TadF pseudopilins, we examined if replacing the signal sequences of pre-TadE and pre-TadF with that of pre-Flp1 would result in functional proteins. Chimeric protein expression constructs were generated by ligating the 5′ end fragment of the *flp-1* gene, containing its Shine-Dalgarno sequence and the first 25 codons, to 5′-end-truncated *tadE* or *tadF* genes, starting with codons G10 and G18, respectively. The resulting constructs, $Flp1_{1\text{-}25}$-$TadE_{10\text{-}191}$ and $Flp1_{1\text{-}25}$-$TadF_{18\text{-}192}$, were termed Flp1-TadE and Flp1-TadF, respectively, and were cloned into the pJAK17 expression vector. Both the *tadE* mutant expressing Flp1-TadE (Aa2575) and the *tadF* strain expressing Flp1-TadF (Aa2579) were capable of forming biofilms in the qualitative adherence assay (see Fig. S1 in the supplemental material). In the quantitative assay both strains exhibited similar levels of adherence to that of the wild-type strain carrying the pJAK17 vector (see Fig. S1). The ability of Flp1-TadE and Flp1-TadF chimeric constructs to restore biofilm formation in the *tadE* and *tadF* mutant strains, respectively, demonstrated that both proteins are functional and are appropriately targeted to the inner membrane and subsequently processed. This conclusion is supported by the observation that only mature TadE protein was detected by anti-TadE immunoblotting when Flp1-TadE was expressed in the *tadE* mutant strain (data not shown).

As the primary structural component of Flp pili (38, 42), the

Flp1 pilin would be expected to be the most abundant protein, relative to other components of the Flp pilus biogenesis apparatus. Comparison of the predicted Shine-Dalgarno sequences upstream of the *flp-1* gene to those of *tadE* and *tadF* is consistent with this prediction. A very strong predicted Shine-Dalgarno sequence was identified upstream of the *flp-1* gene (Fig. 3C) (GenBank accession no. AY157714) that matches exactly the *A. actinomycetemcomitans* Shine-Dalgarno sequence, established by analysis of the 16S rRNA (data not shown). A particularly weak Shine-Dalgarno sequence was identified upstream of the *tadF* gene, while that of the *tadE* gene appeared to be of intermediate strength (Fig. 3C). The sequence analyses of putative Shine-Dalgarno sequences indicate that the expression of Flp1, TadE, and TadF is regulated, at least in part, at the level of translational initiation.

Because the Flp1-TadE and Flp1-TadF chimeric expression constructs both contain the *flp-1* Shine-Dalgarno sequence, it is likely that translational efficiency of the resulting transcripts is increased, relative to those of *tadE* and *tadF* with their native Shine-Dalgarno sequences. Consistent with this prediction, levels of TadE were significantly higher in the *tadE* mutant expressing the Flp1-TadE chimera (Aa2575), compared to preparations from the *tadE* mutant expressing wild-type TadE (Aa2553) (data not shown).

Both *tadE* and *tadF* of *A. actinomycetemcomitans* are essential for Flp pilus biogenesis (40). Given the level of sequence and architectural similarity between the prepseudopilins, we wished to determine if overproduction of either TadE or TadF is sufficient for *A. actinomycetemcomitans* pilus biogenesis. Neither the *tadE* mutant overexpressing TadF (pMT141) nor the *tadF* mutant overproducing TadE (pMT157) was capable of biofilm formation (data not shown). These results show that the *A. actinomycetemcomitans* TadE and TadF proteins, despite having significant similarity, have unique functions in Flp pilus biogenesis.

Processing is required for function of the Flp1 pilin and the TadE and TadF pseudopilins. To determine if processing of the prepilin is required for the function of Flp1 and to help characterize the amino acid residues required for maturation of the pilin, site-directed mutagenesis was utilized to change highly conserved residues within the predicted processing site of Flp1. The glycine and glutamic acid residues, G(−1) and E(+5), respectively, relative to the cleavage site in the prepilin, were replaced with alanine residues. The Flp1 G26A and Flp1 E31A mutant proteins were expressed in the *flp-1* mutant strain JK1010 from plasmid-borne constructs under the control of the *tac*p promoter, and their ability to restore adherence was examined. In the qualitative assay, the Flp1 G26A protein restored adherence of the *flp-1* mutant (Aa2536) (Fig. 5A), allowing it to form biofilms similar to those of the wild-type strain CU1000N harboring the pJAK17 vector (Aa2519) and the *flp-1* mutant strain complemented with the wild-type *flp-1* gene in *trans* (Aa2535). In the quantitative assay, the *flp-1* mutant strain harboring the empty pJAK17 vector (Aa2523) exhibited background levels of biofilm formation, more than 10-fold reduced in comparison to the wild-type strain carrying pJAK17 (Fig. 5B). When grown in the presence of either 0.1 mM or 1 mM IPTG, but not in its absence, the levels of biofilms formed by the *flp-1* mutant strain expressing Flp1 G26A were indistinguishable from those formed by the wild-type strain (Fig. 5B).

We hypothesized that the G26A conservative mutation allowed at least partial processing of Flp1 that resulted in complementation of adherence and biofilm formation. To test this possibility, a whole-cell extract of the *flp-1* mutant harboring the Flp1 G26A expression construct was immunoblotted with anti-Flp1 antiserum, and the relative level and processing state of Flp1 in this strain were compared to those in the *flp-1* mutant expressing wild-type *flp-1* (Aa2535). An abundant band of 7 kDa, corresponding in size to mature Flp1, was detected in preparations of strain Aa2535 grown in the presence of either 0.1 mM or 1 mM IPTG (Fig. 5G). Similar levels of processed Flp1 were detected in whole-cell extracts of strain Aa2536 expressing Flp1 G26A upon induction with IPTG, indicating that Flp1 accumulation correlates with restoration of adherence. Unprocessed pre-Flp1 was not detectable in strain Aa2536, demonstrating that Flp1 G26A is readily processed by TadV.

To further examine the requirement of the glycine residue for processing, we generated a Flp1 G26Y mutant expression construct, containing a more drastic substitution of the glycine residue with tyrosine. The *flp-1* mutant strain expressing Flp1 G26Y (Aa2552) was unable to form visible biofilms in the qualitative adherence assay (Fig. 5A), and it exhibited similar levels of adherence to the *flp-1* mutant with vector control (Aa2523) (Fig. 5B). When examined by anti-Flp1 immunoblotting, a band of approximately 8 kDa was detectable in preparations of strain Aa2552 that corresponded in size to pre-Flp1, while the mature pilin was absent (Fig. 5G). These results demonstrate that the G(−1) residue in the processing site is important for pilin maturation and that proteolytic maturation of Flp1 is essential for Flp pilus biogenesis and biofilm formation.

To determine if processing is also required for function of pre-TadE and pre-TadF, their G(−1) and E(+5) residues were mutated. Substitution of G10 of TadE and G18 of TadF with alanines had no significant effect on the function of either of the proteins, as determined by both the qualitative and quantitative adherence assays (Aa2550 [Fig. 5C and D] and Aa2549 [Fig. 5E and F]). These results indicate that the G(−1)-to-alanine substitutions in the processing sites of pre-TadE and pre-TadF are not sufficient to cause defects in function. The G(−1) residues in the processing sites of both prepseudopilins were also mutated to tyrosine residues. In the qualitative adherence assay, both the *tadE* and the *tadF* mutants expressing TadE G10Y or TadF G18Y, respectively, were defective in biofilm formation (Aa2567 [Fig. 5C] and Aa2563 [Fig. 5E]). Furthermore, these strains were significantly reduced in adherence in the quantitative assay, relative to the mutant strains complemented with wild-type genes (Fig. 5D and F). Immunoblot analysis confirmed that the TadE G10Y protein is expressed in strain Aa2567 but is not processed (data not shown). Such analysis could not be performed for the TadF G18Y protein due to the lack of a TadF-specific antibody. The inability of TadE G10Y and TadF G18Y to restore adherence demonstrates that the G(−1) residue is important for maturation of both proteins and that processing of both pseudopilins is essential for their function.

To examine the role of the conserved E(+5) residue in

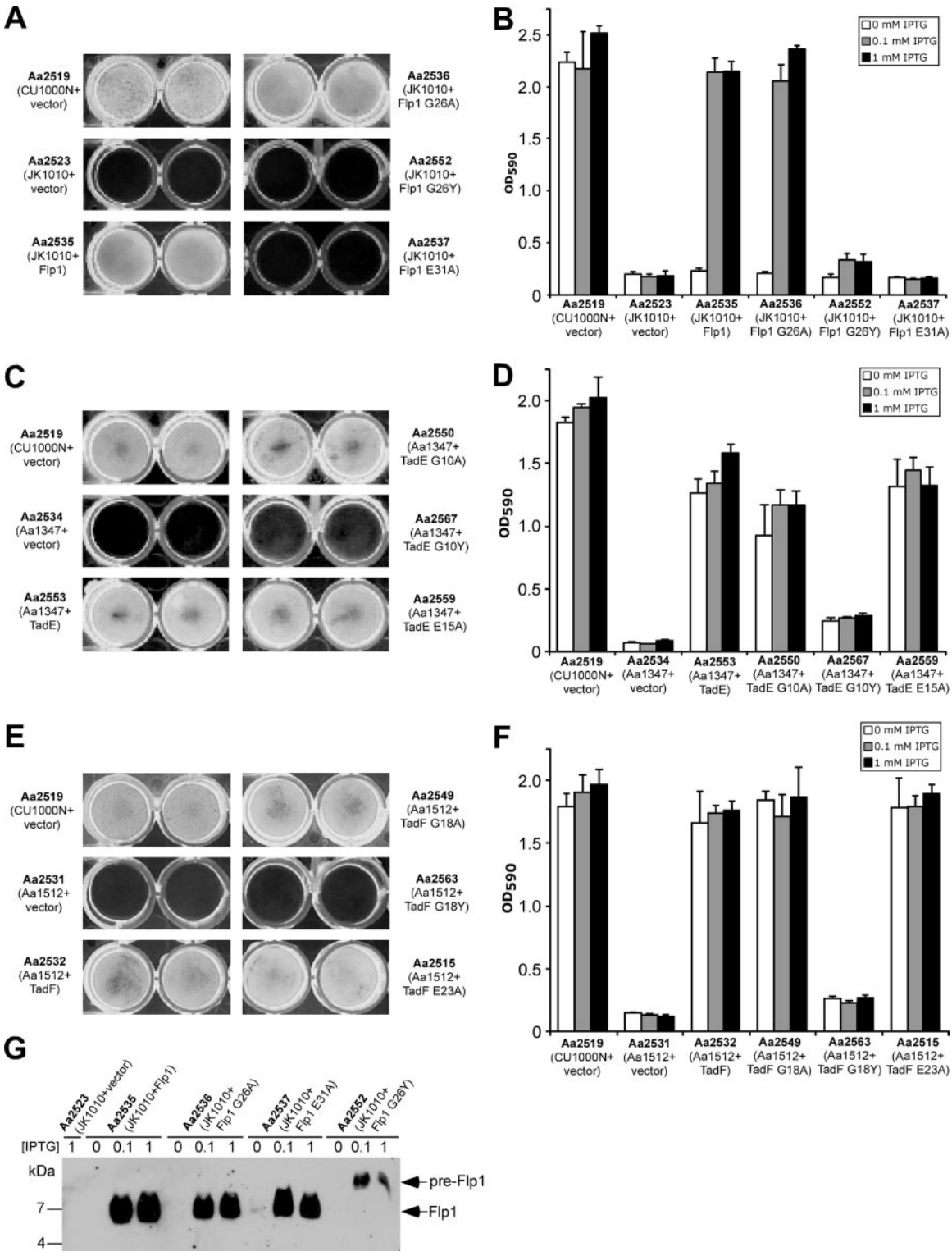

FIG. 5. Analysis of Flp1, TadE, and TadF site-directed mutants. Results from qualitative (A, C, and E) and quantitative (B, D, and F) adherence assays examining the effect of G(−1) and E(+5) mutations on Flp1 (A and B), TadE (C and D), and TadF (E and F) functions are shown. The bars indicate standard deviations. (G) Analysis of mutant Flp1 expression and processing. *A. actinomycetemcomitans* strains were grown in the absence or presence of IPTG, as indicated at the top of the panel. Whole-cell extracts were examined by anti-Flp1 immunoblot analysis. Arrows indicate the positions of the pre-Flp1 and mature Flp1 protein bands.

processing and function of the Flp1 pilin, we tested the ability of strain Aa2537 harboring the Flp1 E31A expression plasmid to form biofilms. Strain Aa2537 did not form visible biofilms in the qualitative adherence assay (Fig. 5A), and its level of biofilm formation in the quantitative assay was indistinguishable from that of the vector control strain (Fig. 5B). To determine whether the defect of the Flp1 E31A mutant is due to instability of the mutant protein or a block in processing, whole-cell extracts of strain Aa2537 were examined by anti-Flp1 immunoblotting. The relative abundance of the Flp1 E31A protein was similar to the amount of wild-type Flp1 detected in the *flp-1* mutant strain complemented with wild-type *flp-1* (Fig. 5G). The Flp1 E31A protein was mature, with no unprocessed prepilin detectable in preparations from strain Aa2537, demonstrating that residue E31 is critical for the function of the Flp1 pilin, but not for its stability or processing.

To examine if the E(+5) residues in the processing sites of pre-TadE and pre-TadF are required for function, TadE E15A and TadF E23A mutant proteins were generated. Immunoblot analysis confirmed both expression and processing of TadE E15A (data not shown). In contrast to our findings in the Flp1 site-directed mutagenesis, the E(+5) mutations in TadE or TadF had no effect on biofilm formation in the qualitative adherence assay (Aa2559 [Fig. 5C] and Aa2515 [Fig. 5E]). Moreover, in the quantitative assay, TadE E15A and TadF E23A were able to restore adherence to the same levels as the wild-type TadE and TadF proteins, respectively (Fig. 5D and F), demonstrating that E(+5) residues are not critical for the function or processing of these proteins.

TadV is a member of a novel subclass of nonmethylating prepilin peptidases. Sequence comparisons of the *A. actinomycetemcomitans* TadV protein with representative homologs encoded by *tad* loci in other organisms demonstrated a significant level of sequence conservation (Fig. 6A), with amino acid similarities ranging between 40% (*C. crescentus* CpaA) and 76% (*P. multocida* TadV). The sequence similarities between *A. actinomycetemcomitans* TadV and representative prepilin peptidases from T2S and T4P systems were markedly lower, ranging from 16% (*Aeromonas hydrophila* TapD) to 22% (enteropathogenic *E. coli* BfpP). We previously demonstrated that the pilus protein secretion systems encoded by *tad* loci are distinct from T2S and T4P systems, while all three systems have diverged from a common, ancestral locus (61, 62). Some of the T2S and T4P proteins are bifunctional enzymes, in which the C-terminal domain of the protein functions as prepilin peptidase, while the N-terminal domain is an *N*-methylase (58, 74). The latter domain is responsible for methylation of phenylalanine residues found at the +1 position in type IVa pilins and/or pilin-like proteins of T4P systems, as well as pseudopilins of T2S systems (63, 74). The *A. actinomycetemcomitans* TadV protein and its homologs encoded by other *tad* loci, including *C. crescentus* CpaA (70), lack an N-terminal methylase domain, indicating that they cannot catalyze transfer of methyl groups. No other gene in the *A. actinomycetemcomitans* *tad* locus, or other known *tad* loci, is predicted to encode an *N*-methylase domain. Furthermore, phenylalanine residues are not found at the +1 position of the *A. actinomycetemcomitans* Flp1 pilin and its homologs (42) or of TadE and TadF pseudopilins (Fig. 3A), strongly indicating that these proteins are not methylated following processing. It therefore appears that the *A. actinomycetemcomitans* TadV protein and its close homologs constitute a novel subclass of prepilin peptidase that lack *N*-methylase activity.

A. actinomycetemcomitans TadV is a 142-amino-acid protein with the predicted molecular mass of 15.8 kDa. Numerous attempts to detect expression of TadV in *A. actinomycetemcomitans* using an affinity-purified anti-$TadV_{116-127}$ peptide antibody were unsuccessful (data not shown). In contrast, the purified antibody was able to detect the TadV peptide immunogen (data not shown), indicating that the TadV protein is expressed at low levels in *A. actinomycetemcomitans*. We also generated C-terminal TadV-T7-tag and TadV-eGFP fusion constructs to examine the expression level of TadV, but these proteins were also undetectable (data not shown). We were therefore unable to examine TadV expression in *A. actinomycetemcomitans*.

The PSORTb 2.0 and TMpred algorithms predicted TadV to localize to the inner membrane. TadV is predicted to lack a cleavable signal sequence and to have five transmembrane segments (TM1 to TM5) (Fig. 6A), which is consistent with its function as a prepilin peptidase as well as with the determined or inferred localization patterns of other known prepilin peptidases (1, 48, 72). The catalytic domains of several T4P and T2S peptidases have been characterized in other systems. In all cases, two invariant catalytic aspartic acid residues are found within broader conserved regions of the T4P and T2S peptidases. The consensus sequences of aspartic acid-containing domains are **D**HXXXH**LP** and H**G**X**GD**H**XL**, in which the residues indicated in bold are absolutely conserved (1, 48).

Sequence analysis of the *A. actinomycetemcomitans* TadV protein and its homologs identified two invariant aspartic acid residues, D23 and D77, which are found within cytoplasmic loops 1 and 2, respectively (Fig. 6B). The aspartic acid residues are flanked by additional highly conserved amino acid residues which appear to be distinct from the consensus sequence reported for the T4P and T2S signal peptidases. Based on our analysis of 14 TadV homologs, including those in Fig. 6A, the consensus sequence of the first aspartic acid-containing domain in this subclass is **D**(I/L)XXRXL, while the consensus for the second domain is (G/A)(G/A)**GD**X**K**L, where bold letters denote invariant residues, plain letters denote residues conserved in at least 85% of the sequences analyzed, and X indicates a nonconserved residue. The distinct consensus sequences of the putative catalytic sites in *A. actinomycetemcomitans* TadV and its homologs confirm that this group represents a novel subclass of prepilin peptidases, which is consistent with a high level of conservation of components encoded by *tad* loci (62).

The predicted membrane topology of TadV (Fig. 6B) strikingly resembles the topology of the *V. cholerae* TcpJ prepilin peptidase domain (48), with TadV lacking the last TcpJ membrane-spanning domain. The organization of the five TM domains of TadV resembles that of the first five membrane-spanning segments of the *Methanococcus voltae* preflagellin peptidase FlaK (5). The positions of the TadV conserved aspartic acid residues, D23 and D77, in cytoplasmic loops 1 and 2, respectively, are similar to the locations of the corresponding catalytic residues in the peptidase domains of TcpJ (48), FlaK (5), and the R64 plasmid-encoded prepilin peptidase PilU (1). The aspartic acid-containing catalytic sites of TadV are predicted to localize on the cytoplasmic face of the inner mem-

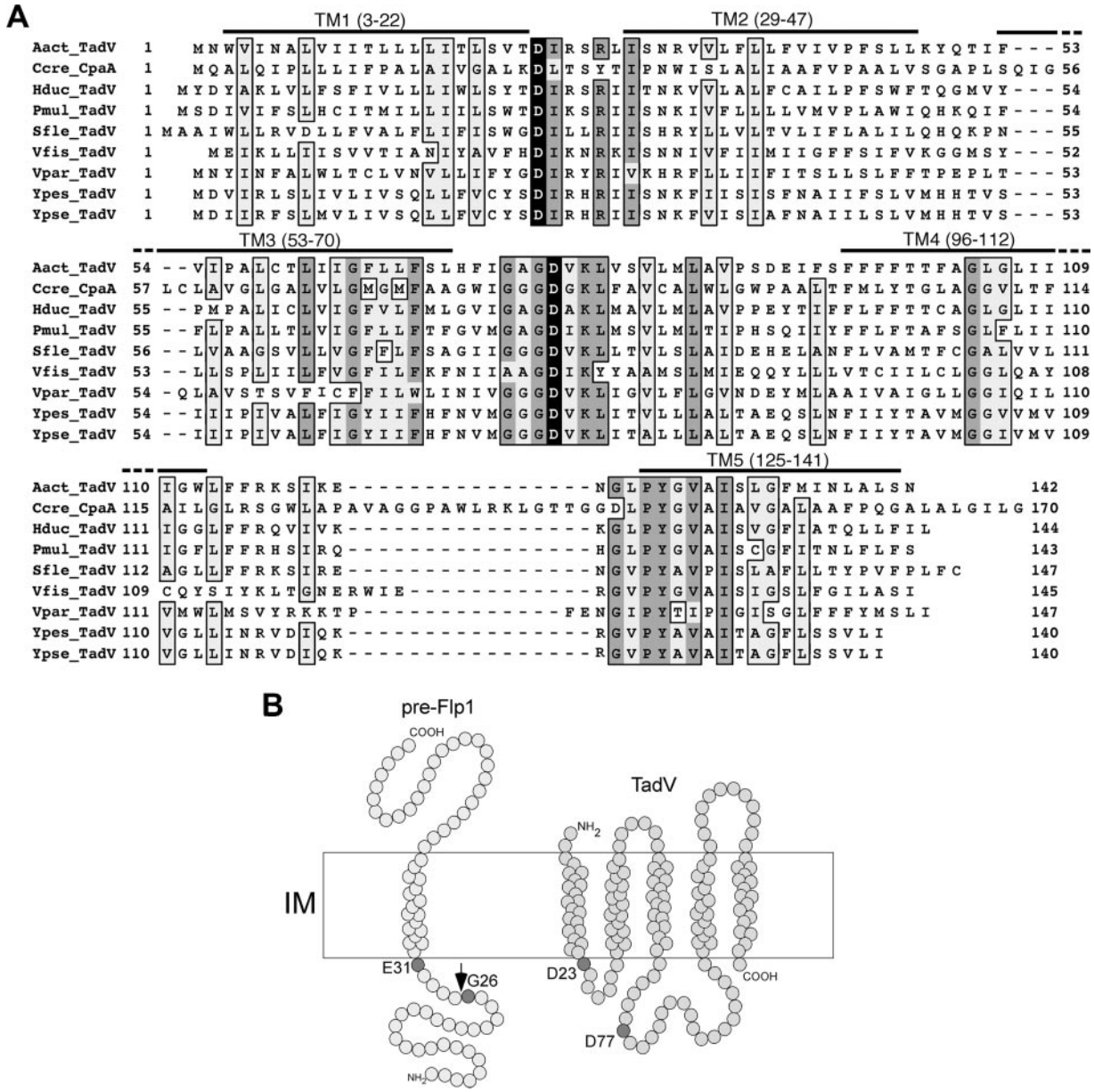

FIG. 6. Amino acid alignment of TadV homologs and the predicted topology of the *A. actinomycetemcomitans* TadV. (A) Identical and similar residues are shown in darkly and lightly shaded boxes, respectively. The highly conserved aspartic acid residues in the predicted catalytic sites are shown in black boxes. The predicted *A. actinomycetemcomitans* TadV transmembrane domains (TM1 to TM5) are indicated with black lines above the amino acid sequence, and the residues that encompass them are indicated in parentheses. Abbreviations: Aact, *A. actinomycetemcomitans*; Ccre, *C. crescentus*; Hduc, *H. ducreyi*; Pmul, *P. multocida*; Sfle, *Shigella flexneri*; Vfis, *Vibrio fischeri*; Vpar, *Vibrio parahaemolyticus*; Ypes, *Y. pestis*, Ypar, *Yersinia paratuberculosis*. (B) Predicted membrane topologies of *A. actinomycetemcomitans* TadV and pre-Flp1 proteins. The TadV catalytic aspartic acid residues are shaded dark gray, as are the residues of pre-Flp1, demarcating the prepilin processing site. The site of cleavage of pre-Flp1 is indicated with the black arrow.

brane (Fig. 6B). Like the pilins of T4P systems, pre-Flp1 is thought to insert into the inner membrane via its N-terminal hydrophobic domain. Colocalization of the prepilin and prepseudopilin N-terminal cleavage sites with the catalytic sites of TadV on the cytoplasmic face of the inner membrane is likely essential for processing (Fig. 6B).

Predicted catalytic aspartic acid residues in *A. actinomycetemcomitans* TadV are critical for function. Having identified the invariant aspartic acid residues in the *A. actinomycetemcomitans* TadV protein, we aimed to determine if they are required for function of the *tad* locus prepilin peptidase. The TadV D23A and TadV D77A mutants were generated using site-directed mutagenesis. In the qualitative adherence assay, like the *tadV* mutant strain carrying the pJAK17 vector (Aa2540), the *tadV* mutant expressing either TadV D23A (Aa2565) or TadV D77A (Aa2561) was unable to form visible biofilms (Fig. 7A). These findings were corroborated by the quantitative adherence assay, in which the *tadV* mutant strain expressing either of

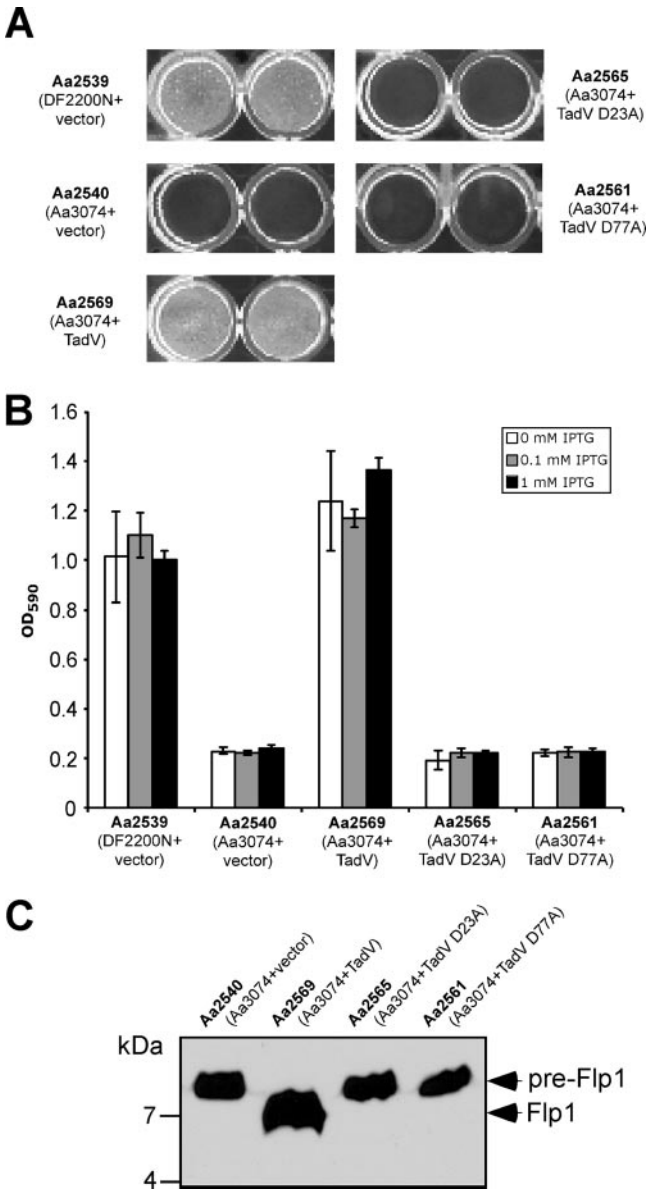

FIG. 7. Functional characterization of the TadV site-directed mutants. (A) Qualitative adherence assay. (B) Quantitative adherence assay. The bars indicate standard deviations. (C) Immunoblot analysis of Flp1 expression and processing. Strains were grown in the presence of 1 mM IPTG. The arrows indicate the positions of the pre-Flp1 and mature Flp1 proteins.

the aspartic acid mutant proteins exhibited adherence levels indistinguishable from the vector control strain, Aa2540 (Fig. 7B). Induction with IPTG was unnecessary to achieve full complementation in strain Aa2569. However, at 1 mM IPTG, adherence of this strain was greater than that of the wild-type strain (Fig. 7B), indicating that overexpression of the prepilin peptidase leads to more efficient processing of the pre-Flp1 pilin and/or the pre-TadE and pre-TadF proteins and results in enhanced pilus morphogenesis. Furthermore, the *tadV* mutant strain expressing either TadV D23A or TadV D77A mutant proteins was unable to process Flp1 (Fig. 7C) and TadE (data not shown). Taken together, these results strongly indicate that the highly conserved aspartic acid residues D23 and D77 are critical for the catalytic function of *A. actinomycetemcomitans* TadV.

DISCUSSION

Here we characterized the function of the *A. actinomycetemcomitans* TadV protein and established that it functions as a prepilin peptidase in maturation of the Flp1 pilin. In addition, we demonstrated that TadV also processes the pre-TadE and pre-TadF proteins. Processing of all three proteins is essential for adherence and biofilm formation by *A. actinomycetemcomitans*. The TadE and TadF proteins appear to be representatives of a novel subclass of bacterial pseudopilins required for pilus biogenesis. We also found that both of the highly conserved aspartic acid residues of the *A. actinomycetemcomitans* TadV protein are critical for its function. Our data strongly indicate that this protein, and its homologs encoded by orthologous *tad* loci, are novel members of a subclass of aspartic acid prepilin peptidases.

The Flp1 pilin has been shown to be glycosylated in at least one strain of *A. actinomycetemcomitans* (37). We found that Flp1 is also glycosylated in *A. actinomycetemcomitans* strain CU1000N (data not shown), which likely accounts for its reduced mobility in SDS-PAGE gels, relative to the predicted molecular mass of 5.1 kDa for the mature pilin (Fig. 2B). Conversely, migration of the processed Flp1 pilin expressed in *E. coli*, which is expected to lack the enzymes required for Flp1 glycosylation, is consistent with the predicted molecular mass of the mature protein (Fig. 2B). The discrepancy in migration further supports the conclusion that Flp1 is modified in *A. actinomycetemcomitans* strain CU1000N, but not in *E. coli*. The mature CU1000N Flp1 pilin migrates as a wide band in SDS-PAGE gels (Fig. 2B and C), possibly due to differential glycosylation levels. Our analysis of *A. actinomycetemcomitans tad* mutants demonstrated that Flp1 from the *rcpC* mutant migrates at a lower molecular mass in SDS-PAGE gels than the processed pilin in other *tad* mutant strains (Fig. 2B). It is possible that the faster migration of Flp1 from the *rcpC* mutant is a result of a complete or partial reduction in pilin glycosylation. It is also tempting to speculate that the RcpC protein, predicted to localize to the inner and/or outer membrane, plays a role in glycosylation of the Flp1 pilin. Conversely, the *rcpC* mutation had no apparent effect on the migration of TadE (Fig. 4B). Future studies will focus on elucidating the molecular mechanism of Flp1 pilin glycosylation in *A. actinomycetemcomitans*.

The crystal structures of *N. gonorrhoeae*, *P. aeruginosa*, and *V. cholerae* T4P pilins demonstrate that the N-terminal hydrophobic domain is packed into the center of the helical pilus structure (14, 55). It is reasonable to propose that the Flp1 pilin monomers are organized similarly within the *A. actinomycetemcomitans* Flp pili. Immunoblot analysis of the Flp pili showed strong interactions between Flp1 monomers (Fig. 2B). Since Flp1 from strain CU1000N lacks cysteine residues, as do its homologs in other prokaryotic *tad* loci (42), the strength of interactions between monomers cannot be attributed to disulfide bonds. It is likely that these interactions are mediated by the N-terminal hydrophobic domain of mature Flp1.

The levels of Flp1 in strains from the *tad* mutant panel were

variable but in all cases were lower than in the wild-type strain CU1000N (Fig. 2C). All *tad* mutants in the panel are blocked in Flp pilus biogenesis (40, 42, 59, 62). Whole-cell extracts prepared from *tad* mutants reflect intracellular levels of Flp1 alone, whereas the preparation of the adherent CU1000N also includes assembled pili attached to the bacterial cells, thus likely increasing the relative abundance of Flp1 in the wild-type strain preparation. It is likely that the *rcpC*, *tadB*, *tadC*, and *tadD* mutants, shown to have an approximately twofold decrease in Flp1 (Fig. 2C), do not have any significant reduction in intracellular Flp1 pilin levels. However, the drastic reduction in the abundance of Flp1 in *rcpA*, *tadZ*, *tadA*, *tadE*, *tadF*, and *tadG* mutant strains (Fig. 2C) is likely due to either direct or indirect effects of the disrupted gene products on Flp1 stability. Given the similarities in architecture of Flp1, TadE, and TadF, it is possible that the pseudopilins directly interact with the pilin.

Levels of the TadE pseudopilin were particularly reduced in the *rcpC* and *rcpA* mutant strains (Fig. 4A). The TadE pseudopilin was not detectable in the *tadF* mutant (Fig. 4A), indicating that TadF may be required for the stability of TadE, and/or that the two pseudopilins interact directly. As the TadF-specific antibody was unavailable, it was not possible to determine the levels of TadF in individual *A. actinomycetemcomitans tad* gene mutants. Nonetheless, since *tadF* is the only gene in the *tad* locus required for TadE expression (Fig. 4A), it is likely that all *tad* mutant strains, with the possible exception of the *tadE*, also express TadF.

The TadF-eGFP fusion protein was expressed, processed, and functional in *A. actinomycetemcomitans* (Fig. 4B and data not shown). However, the fusion protein did not fluoresce in *A. actinomycetemcomitans*. The C terminus of TadF is predicted to localize to the periplasmic space, which is prohibitive of proper folding of GFP (22). The TadE-eGFP and TadV-eGFP fusion proteins also complemented the adherence of the *tadE* and *tadV* mutants, respectively, but did not fluoresce (data not shown). The lack of observed fluorescence of all three fusions is consistent with the predicted localization of pre-TadE and pre-TadF proteins to the inner membrane (Fig. 6B), where they would be processed by the TadV prepilin peptidase. Additional evidence for targeting of the prepseudopilins to the inner membrane is the observed functional interchangeability of their N-terminal signal sequences with that of pre-Flp1 (see Fig. S1 in the supplemental material).

Given the high level of similarity between the two pseudopilins and the requirement of *tadF* for TadE expression (Fig. 4A), it is possible that TadE and TadF directly interact. Recent studies have demonstrated that pseudopilins in other systems, including the *P. aeruginosa* Xcp (21) and *X. campestris* Xps (46) T2S systems, directly interact with each other to facilitate protein secretion. Pseudopilins in a number of T2S systems, including the *K. oxytoca* PulG and the *E. coli* GspG proteins, can form pilus-like oligomeric structures termed pseudopili (66, 78). These findings have supported the hypothesis that pseudopilins in T2S systems of gram-negative bacteria form piston-like structures within the periplasmic space which are thought to facilitate extrusion of the substrate through the outer membrane pore (33). The precise mechanisms by which pseudopilins function in protein secretion systems, and particularly in pilus assembly, remain unclear.

As both TadE and TadF proteins are essential for Flp pilus biogenesis (40), it is likely that each protein plays a unique role in the secretion apparatus. However, the mechanisms by which TadE and TadF function may be, at least in part, conserved. The TadE pseudopilin was not detected in strain CU1000N semipure pilus preparations, indicating that it is not a structural component of Flp pili (data not shown). The highly conserved E(+5) residue in Flp1 is essential for function but not for processing (Fig. 5A and B), while it is dispensable for TadE and TadF function. This glutamic acid residue has been proposed to play a critical role in registering incoming pilin molecules by the growing pilus structure, and T4P pilins with mutated E(+5) residues are blocked in assembly (14, 55, 56, 73).

There are several possible explanations for our observation that TadE and TadF do not require the E(+5) residues. It is possible that the TadE and TadF do not form oligomers and instead function as monomeric proteins. However, we do not favor this hypothesis, since it does not explain the fact that processing of the *A. actinomycetemcomitans* pseudopilins is required for function. It is also possible that TadE and TadF are partially redundant, so that as long one of the pseudopilins is able to form oligomeric complexes through an E(+5)-dependent mechanism, the other one does not need to. If *A. actinomycetemcomitans* pseudopilins interact with each other similarly to pilins and pseudopilins from T4P and/or T2S systems, incorporation of an E(+5) mutant pseudopilin would terminate the extension of the pseudopilus. Interestingly, the PulK pseudopilin in *K. oxytoca* and the XcpX homolog of the *P. aeruginosa* T2S systems lack the E(+5) residue and have been shown to block pseudopilus formation when overexpressed (21, 78). It has been proposed that these proteins regulate the pseudopilus length by terminating its elongation (21, 78). It is also formally possible that the E(+5) residues in TadE and TadF are dispensable for polymerization, although this possibility is unlikely, as it does not explain the high level of conservation of the E(+5) residue in TadE and TadF pseudopilins (Fig. 3A).

The tyrosine residue at position +6 of Flp1 is also highly conserved among Flp homologs (42). We have recently determined that the *A. actinomycetemcomitans* Y(+6) residue is critical for biofilm formation (V. Grosso and D. H. Figurski, unpublished data). Interestingly, the Y(+6) residue is absent in the TadE and TadF pseudopilins, highlighting another distinction between the biology of the Flp1 pilin and that of the pseudopilins.

The *A. actinomycetemcomitans* TadV protein is a member of a novel subclass of nonmethylating prepilin peptidases, which we have previously demonstrated to be widespread in prokaryotes (62). We showed that both of the highly conserved aspartic acid residues in TadV are essential for function (Fig. 6 and 7). A very recent report has shown that the conserved aspartic acid residues are also important for FppA-dependent maturation of the *P. aeruginosa* Flp pilin (15). As we were unable to detect TadV expression in *A. actinomycetemcomitans*, it is formally possible that the D23A and D77A mutations in the prepilin peptidase resulted in instability, which would also explain the lack of complementation of the *tadV* mutant (Fig. 7). However, site-directed mutagenesis of the corresponding aspartic acid residues in a number of homologous proteins from other systems, including *V. cholerae* TcpJ and

VcpD proteins (48) and the PibD preflagellin peptidase of the archaeon *Sulfolobus solfataricus* (76), had no effect on peptidase stability or localization. Moreover, extensive mutagenesis of other residues in predicted cytoplasmic loops of TcpJ, VcpD, and PibD had no significant effects on stability (48, 76). As the *A. actinomycetemcomitans* TadV residues D23 and D77 are predicted to be within cytoplasmic loops (Fig. 6), it is highly unlikely that their individual replacement with alanines would lead to destabilization or mislocalization of the protein. Our results strongly indicate that the TadV protein of *A. actinomycetemcomitans* is an aspartic acid peptidase required for processing of the Flp1 pilin and the TadE and TadF pseudopilins. Future studies in our laboratory will continue to dissect the structure and function of the Flp pilus secretion apparatus.

ACKNOWLEDGMENTS

We thank Scott Kachlany for constructing plasmid pSK305 and John Berriman at the New York Structural Biology Center and Yoram Puius for assistance with electron microscopy. We thank Jeff Kaplan for providing the protocol for Flp pilus purification. We are grateful to the members of the Figurski laboratory, especially Brenda Perez, as well as Paul Planet, Howard Shuman, and Jonathan Dworkin for helpful discussions. We also thank Saul Silverstein and Aaron Mitchell for their assistance.

This work was supported by NIH grant 5R01DE014713 to D. H. Figurski.

REFERENCES

1. **Akahane, K., D. Sakai, N. Furuya, and T. Komano.** 2005. Analysis of the *pilU* gene for the prepilin peptidase involved in the biogenesis of type IV pili encoded by plasmid R64. Mol. Genet. Genomics **273:**350–359.
2. **Albers, S. V., Z. Szabo, and A. J. Driessen.** 2003. Archaeal homolog of bacterial type IV prepilin signal peptidases with broad substrate specificity. J. Bacteriol. **185:**3918–3925.
3. **Armitage, G. C.** 1999. Development of a classification system for periodontal diseases and conditions. Ann. Periodontol. **4:**1–6.
4. **Asikainen, S., S. Alaluusua, and L. Saxen.** 1991. Recovery of *A. actinomycetemcomitans* from teeth, tongue, and saliva. J. Periodontol. **62:**203–206.
5. **Bardy, S. L., and K. F. Jarrell.** 2003. Cleavage of preflagellins by an aspartic acid signal peptidase is essential for flagellation in the archaeon *Methanococcus voltae*. Mol. Microbiol. **50:**1339–1347.
6. **Bardy, S. L., and K. F. Jarrell.** 2002. FlaK of the archaeon *Methanococcus maripaludis* possesses preflagellin peptidase activity. FEMS Microbiol. Lett. **208:**53–59.
7. **Bhattacharjee, M. K., S. C. Kachlany, D. H. Fine, and D. H. Figurski.** 2001. Nonspecific adherence and fibril biogenesis by *Actinobacillus actinomycetemcomitans*: TadA protein is an ATPase. J. Bacteriol. **183:**5927–5936.
8. **Bleves, S., R. Voulhoux, G. Michel, A. Lazdunski, J. Tommassen, and A. Filloux.** 1998. The secretion apparatus of *Pseudomonas aeruginosa*: identification of a fifth pseudopilin, XcpX (GspK family). Mol. Microbiol. **27:**31–40.
9. **Chalfie, M., Y. Tu, G. Euskirchen, W. W. Ward, and D. C. Prasher.** 1994. Green fluorescent protein as a marker for gene expression. Science **263:**802–805.
10. **Chen, I., P. J. Christie, and D. Dubnau.** 2005. The ins and outs of DNA transfer in bacteria. Science **310:**1456–1460.
11. **Chung, Y. S., F. Breidt, and D. Dubnau.** 1998. Cell surface localization and processing of the ComG proteins, required for DNA binding during transformation of *Bacillus subtilis*. Mol. Microbiol. **29:**905–913.
12. **Chung, Y. S., and D. Dubnau.** 1995. ComC is required for the processing and translocation of comGC, a pilin-like competence protein of *Bacillus subtilis*. Mol. Microbiol. **15:**543–551.
13. **Cohen, S. N., A. C. Chang, and L. Hsu.** 1972. Nonchromosomal antibiotic resistance in bacteria: genetic transformation of Escherichia coli by R-factor DNA. Proc. Natl. Acad. Sci. USA **69:**2110–2114.
14. **Craig, L., R. K. Taylor, M. E. Pique, B. D. Adair, A. S. Arvai, M. Singh, S. J. Lloyd, D. S. Shin, E. D. Getzoff, M. Yeager, K. T. Forest, and J. A. Tainer.** 2003. Type IV pilin structure and assembly: X-ray and EM analyses of *Vibrio cholerae* toxin-coregulated pilus and *Pseudomonas aeruginosa* PAK pilin. Mol. Cell **11:**1139–1150.
15. **de Bentzmann, S., M. Aurouze, G. Ball, and A. Filloux.** 2006. FppA, a novel *Pseudomonas aeruginosa* prepilin peptidase involved in assembly of type IVb pili. J. Bacteriol. **188:**4851–4860.
16. **De Marco, V., G. Stier, S. Blandin, and A. de Marco.** 2004. The solubility and stability of recombinant proteins are increased by their fusion to NusA. Biochem. Biophys. Res. Commun. **322:**766–771.
17. **Deng, W., V. Burland, G. Plunkett III, A. Boutin, G. F. Mayhew, P. Liss, N. T. Perna, D. J. Rose, B. Mau, S. Zhou, D. C. Schwartz, J. D. Fetherston, L. E. Lindler, R. R. Brubaker, G. V. Plano, S. C. Straley, K. A. McDonough, M. L. Nilles, J. S. Matson, F. R. Blattner, and R. D. Perry.** 2002. Genome sequence of *Yersinia pestis* KIM. J. Bacteriol. **184:**4601–4611.
18. **Dubnau, D.** 1997. Binding and transport of transforming DNA by *Bacillus subtilis*: the role of type-IV pilin-like proteins—a review. Gene **192:**191–198.
19. **Dubnau, D.** 1999. DNA uptake in bacteria. Annu. Rev. Microbiol. **53:**217–244.
20. **Dupuy, B., and A. P. Pugsley.** 1994. Type IV prepilin peptidase gene of *Neisseria gonorrhoeae* MS11: presence of a related gene in other piliated and nonpiliated *Neisseria* strains. J. Bacteriol. **176:**1323–1331.
21. **Durand, E., G. Michel, R. Voulhoux, J. Kurner, A. Bernadac, and A. Filloux.** 2005. XcpX controls biogenesis of the *Pseudomonas aeruginosa* XcpT-containing pseudopilus. J. Biol. Chem. **280:**31378–31389.
22. **Feilmeier, B. J., G. Iseminger, D. Schroeder, H. Webber, and G. J. Phillips.** 2000. Green fluorescent protein functions as a reporter for protein localization in *Escherichia coli*. J. Bacteriol. **182:**4068–4076.
23. **Fernandez, L., I. Marquez, and J. A. Guijarro.** 2004. Identification of specific in vivo-induced (*ivi*) genes in *Yersinia ruckeri* and analysis of ruckerbactin, a catecholate siderophore iron acquisition system. Appl. Environ. Microbiol. **70:**5199–5207.
24. **Filloux, A.** 2004. The underlying mechanisms of type II protein secretion. Biochim. Biophys. Acta **1694:**163–179.
25. **Fine, D. H., D. Furgang, J. Kaplan, J. Charlesworth, and D. H. Figurski.** 1999. Tenacious adhesion of *Actinobacillus actinomycetemcomitans* strain CU1000 to salivary-coated hydroxyapatite. Arch. Oral Biol. **44:**1063–1076.
26. **Fuller, T. E., M. J. Kennedy, and D. E. Lowery.** 2000. Identification of *Pasteurella multocida* virulence genes in a septicemic mouse model using signature-tagged mutagenesis. Microb. Pathog. **29:**25–38.
27. **Gardy, J. L., M. R. Laird, F. Chen, S. Rey, C. J. Walsh, M. Ester, and F. S. Brinkman.** 2005. PSORTb v. 2.0: expanded prediction of bacterial protein subcellular localization and insights gained from comparative proteome analysis. Bioinformatics **21:**617–623.
28. **Goncharoff, P., J. K. Yip, H. Wang, H. C. Schreiner, J. A. Pai, D. Furgang, R. H. Stevens, D. H. Figurski, and D. H. Fine.** 1993. Conjugal transfer of broad-host-range incompatibility group P and Q. plasmids from *Escherichia coli* to *Actinobacillus actinomycetemcomitans*. Infect. Immun. **61:**3544–3547.
29. **Haase, E. M., J. L. Zmuda, and F. A. Scannapieco.** 1999. Identification and molecular analysis of rough-colony-specific outer membrane proteins of *Actinobacillus actinomycetemcomitans*. Infect. Immun. **67:**2901–2908.
30. **Henderson, B., S. P. Nair, J. M. Ward, and M. Wilson.** 2003. Molecular pathogenicity of the oral opportunistic pathogen *Actinobacillus actinomycetemcomitans*. Annu. Rev. Microbiol. **57:**29–55.
31. **Hilbi, H., G. Segal, and H. A. Shuman.** 2001. Icm/dot-dependent upregulation of phagocytosis by *Legionella pneumophila*. Mol. Microbiol. **42:**603–617.
32. **Ho, S. N., H. D. Hunt, R. M. Horton, J. K. Pullen, and L. R. Pease.** 1989. Site-directed mutagenesis by overlap extension using the polymerase chain reaction. Gene **77:**51–59.
33. **Hobbs, M., and J. S. Mattick.** 1993. Common components in the assembly of type 4 fimbriae, DNA transfer systems, filamentous phage and protein-secretion apparatus: a general system for the formation of surface-associated protein complexes. Mol. Microbiol. **10:**233–243.
34. **Hofmann, K., and W. Stoffel.** 1993. TMbase: a database of membrane spanning protein segments. Biol. Chem. Hoppe-Seyler **374:**166.
35. **Holt, S. C., A. C. Tanner, and S. S. Socransky.** 1980. Morphology and ultrastructure of oral strains of *Actinobacillus actinomycetemcomitans* and *Haemophilus aphrophilus*. Infect. Immun. **30:**588–600.
36. **Hu, N. T., W. M. Leu, M. S. Lee, A. Chen, S. C. Chen, Y. L. Song, and L. Y. Chen.** 2002. XpsG, the major pseudopilin in *Xanthomonas campestris* pv. campestris, forms a pilus-like structure between cytoplasmic and outer membranes. Biochem. J. **365:**205–211.
37. **Inoue, T., H. Ohta, I. Tanimoto, R. Shingaki, and K. Fukui.** 2000. Heterogeneous post-translational modification of *Actinobacillus actinomycetemcomitans* fimbrillin. Microbiol. Immunol. **44:**715–718.
38. **Inoue, T., I. Tanimoto, H. Ohta, K. Kato, Y. Murayama, and K. Fukui.** 1998. Molecular characterization of low-molecular-weight component protein, Flp, in *Actinobacillus actinomycetemcomitans* fimbriae. Microbiol. Immunol. **42:**253–258.
39. **Johnson, T. L., J. Abendroth, W. G. Hol, and M. Sandkvist.** 2006. Type II secretion: from structure to function. FEMS Microbiol. Lett. **255:**175–186.
40. **Kachlany, S. C., P. J. Planet, M. K. Bhattacharjee, E. Kollia, R. DeSalle, D. H. Fine, and D. H. Figurski.** 2000. Nonspecific adherence by *Actinobacillus actinomycetemcomitans* requires genes widespread in bacteria and archaea. J. Bacteriol. **182:**6169–6176.
41. **Kachlany, S. C., P. J. Planet, R. DeSalle, D. H. Fine, and D. H. Figurski.** 2001. Genes for tight adherence of *Actinobacillus actinomycetemcomitans*: from plaque to plague to pond scum. Trends Microbiol. **9:**429–437.
42. **Kachlany, S. C., P. J. Planet, R. Desalle, D. H. Fine, D. H. Figurski, and J. B. Kaplan.** 2001. *flp-1*, the first representative of a new pilin gene subfamily, is required for non-specific adherence of *Actinobacillus actinomycetemcomitans*. Mol. Microbiol. **40:**542–554.

43. **Kaplan, J. B., C. Ragunath, N. Ramasubbu, and D. H. Fine.** 2003. Detachment of *Actinobacillus actinomycetemcomitans* biofilm cells by an endogenous beta-hexosaminidase activity. J. Bacteriol. **185:**4693–4698.
44. **Kaplan, J. B., H. C. Schreiner, D. Furgang, and D. H. Fine.** 2002. Population structure and genetic diversity of *Actinobacillus actinomycetemcomitans* strains isolated from localized juvenile periodontitis patients. J. Clin. Microbiol. **40:**1181–1187.
45. **Kaufman, M. R., J. M. Seyer, and R. K. Taylor.** 1991. Processing of TCP pilin by TcpJ typifies a common step intrinsic to a newly recognized pathway of extracellular protein secretion by gram-negative bacteria. Genes Dev. **5:**1834–1846.
46. **Kuo, W. W., H. W. Kuo, C. C. Cheng, H. L. Lai, and L. Y. Chen.** 2005. Roles of the minor pseudopilins, XpsH, XpsI and XpsJ, in the formation of XpsG-containing pseudopilus in *Xanthomonas campestris* pv. campestris. J. Biomed. Sci. **12:**587–599.
47. **Laemmli, U. K.** 1970. Cleavage of structural proteins during the assembly of the head of bacteriophage T4. Nature **227:**680–685.
48. **LaPointe, C. F., and R. K. Taylor.** 2000. The type 4 prepilin peptidases comprise a novel family of aspartic acid proteases. J. Biol. Chem. **275:**1502–1510.
49. **Lu, H. M., S. T. Motley, and S. Lory.** 1997. Interactions of the components of the general secretion pathway: role of *Pseudomonas aeruginosa* type IV pilin subunits in complex formation and extracellular protein secretion. Mol. Microbiol. **25:**247–259.
50. **Mattick, J. S.** 2002. Type IV pili and twitching motility. Annu. Rev. Microbiol. **56:**289–314.
51. **May, B. J., Q. Zhang, L. L. Li, M. L. Paustian, T. S. Whittam, and V. Kapur.** 2001. Complete genomic sequence of *Pasteurella multocida*, Pm70. Proc. Natl. Acad. Sci. USA **98:**3460–3465.
52. **Meyer, D. H., and P. M. Fives-Taylor.** 1998. Oral pathogens: from dental plaque to cardiac disease. Curr. Opin. Microbiol. **1:**88–95.
53. **Newman, J. R., and C. Fuqua.** 1999. Broad-host-range expression vectors that carry the L-arabinose-inducible *Escherichia coli araBAD* promoter and the *araC* regulator. Gene **227:**197–203.
54. **O'Toole, G. A., and R. Kolter.** 1998. Initiation of biofilm formation in *Pseudomonas fluorescens* WCS365 proceeds via multiple, convergent signalling pathways: a genetic analysis. Mol. Microbiol. **28:**449–461.
55. **Parge, H. E., K. T. Forest, M. J. Hickey, D. A. Christensen, E. D. Getzoff, and J. A. Tainer.** 1995. Structure of the fibre-forming protein pilin at 2.6 Å resolution. Nature **378:**32–38.
56. **Pasloske, B. L., D. G. Scraba, and W. Paranchych.** 1989. Assembly of mutant pilins in *Pseudomonas aeruginosa*: formation of pili composed of heterologous subunits. J. Bacteriol. **171:**2142–2147.
57. **Peabody, C. R., Y. J. Chung, M. R. Yen, D. Vidal-Ingigliardi, A. P. Pugsley, and M. H. Saier, Jr.** 2003. Type II protein secretion and its relationship to bacterial type IV pili and archaeal flagella. Microbiology **149:**3051–3072.
58. **Pepe, J. C., and S. Lory.** 1998. Amino acid substitutions in PilD, a bifunctional enzyme of *Pseudomonas aeruginosa*. Effect on leader peptidase and N-methyltransferase activities in vitro and in vivo. J. Biol. Chem. **273:**19120–19129.
59. **Perez, B. A., P. J. Planet, S. C. Kachlany, M. Tomich, D. H. Fine, and D. F. Figurski.** 2006. Genetic analysis of the requirement for *flp-2*, *tadV*, and *rcpB* in *Actinobacillus actinomycetemcomitans* biofilm formation. J. Bacteriol. **188:**6361–6375.
60. **Planet, P. J.** 2003. The history and function of the widespread colonization island of *Actinobacillus actinomycetemcomitans*. Ph.D. thesis, Columbia University, New York, N.Y.
61. **Planet, P. J., S. C. Kachlany, R. DeSalle, and D. H. Figurski.** 2001. Phylogeny of genes for secretion NTPases: identification of the widespread *tadA* subfamily and development of a diagnostic key for gene classification. Proc. Natl. Acad. Sci. USA **98:**2503–2508.
62. **Planet, P. J., S. C. Kachlany, D. H. Fine, R. DeSalle, and D. H. Figurski.** 2003. The widespread colonization island of *Actinobacillus actinomycetemcomitans*. Nat. Genet. **34:**193–198.
63. **Pugsley, A. P.** 1993. Processing and methylation of PuIG, a pilin-like component of the general secretory pathway of *Klebsiella oxytoca*. Mol. Microbiol. **9:**295–308.
64. **Pugsley, A. P., and B. Dupuy.** 1992. An enzyme with type IV prepilin peptidase activity is required to process components of the general extracellular protein secretion pathway of *Klebsiella oxytoca*. Mol. Microbiol. **6:**751–760.
65. **Sambrook, J., E. F. Fritsch, and T. Maniatis.** 1989. Molecular cloning: a laboratory manual, 2nd ed. Cold Spring Harbor Laboratory Press, Cold Spring Harbor, N.Y.
66. **Sauvonnet, N., G. Vignon, A. P. Pugsley, and P. Gounon.** 2000. Pilus formation and protein secretion by the same machinery in *Escherichia coli*. EMBO J. **19:**2221–2228.
67. **Schoolnik, G. K.** 1994. Purification of somatic pili. Methods Enzymol. **236:**271–282.
68. **Schreiner, H. C., K. Sinatra, J. B. Kaplan, D. Furgang, S. C. Kachlany, P. J. Planet, B. A. Perez, D. H. Figurski, and D. H. Fine.** 2003. Tight-adherence genes of *Actinobacillus actinomycetemcomitans* are required for virulence in a rat model. Proc. Natl. Acad. Sci. USA **100:**7295–7300.
69. **Sia, E. A., D. M. Kuehner, and D. H. Figurski.** 1996. Mechanism of retrotransfer in conjugation: prior transfer of the conjugative plasmid is required. J. Bacteriol. **178:**1457–1464.
70. **Skerker, J. M., and L. Shapiro.** 2000. Identification and cell cycle control of a novel pilus system in *Caulobacter crescentus*. EMBO J. **19:**3223–3234.
71. **Spinola, S. M., K. R. Fortney, B. P. Katz, J. L. Latimer, J. R. Mock, M. Vakevainen, and E. J. Hansen.** 2003. *Haemophilus ducreyi* requires an intact *flp* gene cluster for virulence in humans. Infect. Immun. **71:**7178–7182.
72. **Strom, M. S., P. Bergman, and S. Lory.** 1993. Identification of active-site cysteines in the conserved domain of PilD, the bifunctional type IV pilin leader peptidase/N-methyltransferase of *Pseudomonas aeruginosa*. J. Biol. Chem. **268:**15788–15794.
73. **Strom, M. S., and S. Lory.** 1991. Amino acid substitutions in pilin of *Pseudomonas aeruginosa*. Effect on leader peptide cleavage, amino-terminal methylation, and pilus assembly. J. Biol. Chem. **266:**1656–1664.
74. **Strom, M. S., D. N. Nunn, and S. Lory.** 1993. A single bifunctional enzyme, PilD, catalyzes cleavage and N-methylation of proteins belonging to the type IV pilin family. Proc. Natl. Acad. Sci. USA **90:**2404–2408.
75. **Strom, M. S., D. N. Nunn, and S. Lory.** 1994. Posttranslational processing of type IV prepilin and homologs by PilD of *Pseudomonas aeruginosa*. Methods Enzymol. **235:**527–540.
76. **Szabo, Z., S. V. Albers, and A. J. Driessen.** 2006. Active-site residues in the type IV prepilin peptidase homologue PibD from the archaeon *Sulfolobus solfataricus*. J. Bacteriol. **188:**1437–1443.
77. **Van Winkelhoff, A. J., and J. Slots.** 1999. *Actonobacillus actinomycetemcomitans* and *Porphyromonas gingivalis* in nonoral infections. Periodontology **20:**122–135.
78. **Vignon, G., R. Kohler, E. Larquet, S. Giroux, M. C. Prevost, P. Roux, and A. P. Pugsley.** 2003. Type IV-like pili formed by the type II secreton: specificity, composition, bundling, polar localization, and surface presentation of peptides. J. Bacteriol. **185:**3416–3428.